The Astrophysical Journal Supplement Series, 178:71–88, 2008 September


# IMPROVED LABORATORY TRANSITION PROBABILITIES FOR Er II AND APPLICATION TO THE ERBIUM ABUNDANCES OF THE SUN AND FIVE *r*-PROCESS-RICH, METAL-POOR STARS

J. E. Lawler,[1] C. Sneden,[2] J. J. Cowan,[3] J.-F. Wyart,[4] I. I. Ivans,[5]
J. S. Sobeck,[2] M. H. Stockett,[1] and E. A. Den Hartog[1]

*Received 2008 March 26; accepted 2008 April 22*

## ABSTRACT

Recent radiative lifetime measurements accurate to ±5% (Stockett et al. 2007, J. Phys. B 40, 4529) using laser-induced fluorescence (LIF) on 7 even-parity and 63 odd-parity levels of Er II have been combined with new branching fractions measured using a Fourier transform spectrometer (FTS) to determine transition probabilities for 418 lines of Er II. This work moves Er II onto the growing list of rare-earth spectra with extensive and accurate modern transition probability measurements using LIF plus FTS data. This improved laboratory data set has been used to determine a new solar photospheric Er abundance, $\log \varepsilon = 0.96 \pm 0.03$ ($\sigma = 0.06$ from 8 lines), a value in excellent agreement with the recommended meteoritic abundance, $\log \varepsilon = 0.95 \pm 0.03$. Revised Er abundances have also been derived for the *r*-process-rich metal-poor giant stars CS 22892−052, BD +17 3248, HD 221170, HD 115444, and CS 31082−001. For these five stars the average Er/Eu abundance ratio, $\langle \log \varepsilon(\mathrm{Er/Eu}) \rangle = 0.42$, is in very good agreement with the solar-system *r*-process ratio. This study has further strengthened the finding that *r*-process nucleosynthesis in the early Galaxy, which enriched these metal-poor stars, yielded a very similar pattern to the *r*-process, which enriched later stars including the Sun.

*Subject headings:* atomic data — Galaxy: evolution — nuclear reactions, nucleosynthesis, abundances — stars: abundances — stars: Population II — stars: individual (HD 115444, HD 221170, BD +17 3248, CS 22892−052, CS 31082−001, CS 29497−030) — Sun: abundances

*Online material:* machine-readable table

## 1. INTRODUCTION

The study of elemental abundances in stellar photospheres continues to be a rich area of investigation. The availability of new large-aperture telescopes has dramatically increased the number of target stars for which high spectral resolution data with a high signal-to-noise ratio can be obtained. One of the major successes in this area during recent years was the discovery and detailed study of a class of metal-poor Galactic halo stars with variable *n*-capture (neutron-capture) elemental abundances (e.g., Smith et al. 1995; Sneden et al. 1995, 1996, 2000; Cowan et al. 1996; Woolf et al. 1995; Burris et al. 2000). Halo stars are among the oldest objects in the Galaxy and provide a window on the earliest phases of Galactic evolution. The last decade has seen the first detection and abundance determination of numerous heavy elements in very metal-poor, *n*-capture-rich halo stars, including the important chronometer uranium (Cayrel et al. 2001; Frebel et al. 2007).

Rare-earth (RE) elements are among the most spectroscopically accessible of the *n*-capture elements. The open *f*-shell of the RE neutral atoms and ions yields many strong lines in the visible and near-IR, where spectral line blending is less of a problem than in the UV. Advantages from reduced blending in astrophysical data analysis are not matched by ease in calculating the basic atomic data needed for abundance determinations. These species with open *f*-shells have substantial relativistic effects causing a nearly complete breakdown of Russell-Saunders coupling.[6] They also have many low-lying, overlapping configurations leading to extensive configuration interaction. In some cases there are hundreds to thousands of interacting levels that need to be included in accurate calculations on the strongest "resonance-like" transitions. Ab initio quantum mechanical calculations on these spectra represent a formidable task even with the best currently available computers. The challenge of calculating spectroscopic data for RE neutral atoms and ions has attracted the attention of theorists (see Biémont & Quinet 2003 and references therein). In such complex spectra, progress is being made through an interplay of theory and experiment. Often some experimental information is essential to "tune" theoretical methods.

The systematic determination of experimental transition probabilities by combining radiative lifetimes from time-resolved laser-induced fluorescence (TR-LIF) with branching fractions from emission data recorded with a Fourier transform spectrometer (FTS) has played a central role in providing the basic atomic data needed for RE abundance determinations (e.g., Lawler et al. 2006 and references therein). This method yields absolute transition probabilities that are accurate to ±5% (∼0.02 dex) for

[1] Department of Physics, University of Wisconsin, Madison, WI 53706; jelawler@wisc.edu , stockett@wisc.edu, eadenhar@wisc.edu.

[2] Homer L. Dodge Department of Astronomy and McDonald Observatory, University of Texas, Austin, TX 78712; chris@verdi.as.utexas.edu, jsobeck@astro.as.utexas.edu.

[3] Department of Physics and Astronomy, University of Oklahoma, Norman, OK 73019; cowan@nhn.ou.edu.

[4] Laboratoire Aimé Cotton, Centre National de la Recherche Scientifique (UPR3321), 91405-Orsay, France; jean-francois.wyart@lac.u-psud.fr.

[5] The Observatories of the Carnegie Institution of Washington, 813 Santa Barbara Street, Pasadena, CA 91101 & Princeton University Observatory, Peyton Hall, Princeton, NJ 08544; iii@ociw.edu.

[6] Russell-Saunders coupling applies for light atoms in which the Coulomb repulsion of electrons in the Hamiltonian overwhelms relativistic effects including spin-orbit, spin-other orbit, spin-spin, and orbit-orbit interactions. In most levels of light atoms the total electronic angular momentum operator $\boldsymbol{L}^2$ and total electronic spin $\boldsymbol{S}^2$ are diagonal, or yield very good quantum numbers. In RE atoms relativistic effects are typically comparable to, or larger than, Coulomb repulsion terms in the Hamiltonian. The only generally good quantum numbers for levels of light atoms and RE atoms are eigenvalues of the total electronic angular momentum $\boldsymbol{J}^2 = (\boldsymbol{L} + \boldsymbol{S})^2$ and parity operators.

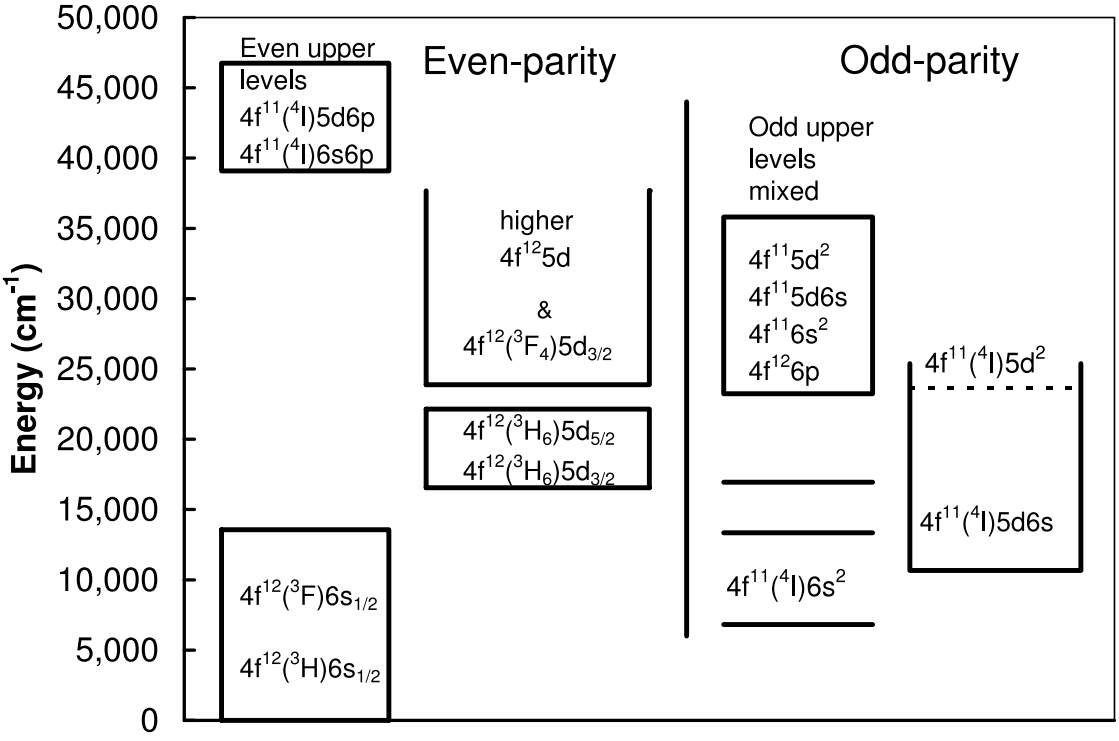


FIG. 1.—Partial Grotrian diagram for Er II. Upper and lower levels of both parities included in this study are shown.

strong lines. Improved laboratory data have reduced line-to-line and star-to-star scatter in abundance values for many RE elements. The emergence of a tightly defined *r*-process-only abundance pattern in many very metal poor Galactic halo stars, at least for the RE elements, has been an exciting development (e.g., Sneden et al. 2003; Ivans et al. 2006; Lawler et al. 2006; Den Hartog et al. 2006). As this abundance pattern becomes even more tightly defined, it will (1) provide a powerful constraint on future modeling of the *r*-process nucleosynthesis; (2) help determine a definitive *r*-process site; and (3) unlock other details of the *r*-process and of the Galactic chemical evolution.

Erbium is one of the RE elements in need of additional work. There have been some LIF lifetime measurements (e.g., Bentzen et al. 1982; Xu et al. 2003, 2004), but a large set of experimental transition probabilities based on the best modern methods was not available before this work. Recent and extensive TR-LIF lifetime measurements by Stockett et al. (2007) provide a foundation for determining a large set of atomic transition probabilities from FTS data. We report the measurement of branching fractions for 418 lines of Er II and the determination of absolute transition probabilities for these lines by combining our branching fractions with radiative lifetime data from Stockett et al. (2007). These laboratory data are applied to redetermine the Solar abundance of Er and to refine the Er abundance in five *r*-process-rich, metal-poor Galactic halo stars.

## 2. Er II BRANCHING FRACTIONS AND ATOMIC TRANSITION PROBABILITIES

The availability of a large and accurate set of radiative lifetimes from Stockett et al. (2007) provides a foundation for this study of branching fractions and the transition probabilities of Er II. A very powerful spectrometer is essential for branching fraction measurements on rich RE spectra. As in earlier work on RE spectra, we used the 1.0 m FTS at the National Solar Observatory (NSO) for branching fraction measurements in this project. This instrument has the large etendue of all interferometric spectrometers, a limit of resolution as small as 0.01 $cm^{-1}$, wavenumber accuracy to 1 part in $10^8$, broad spectral coverage from the UV to IR, and the capability of recording a million point spectrum in 10 minutes (Brault 1976). An FTS is insensitive to any small drift in source intensity since an interferogram is a simultaneous measurement of all spectral lines.

### 2.1. *Energy Levels of* Er II

One of the challenges in this undertaking is the lack of configuration and term assignments for most observed levels of Er II. Figure 1 shows a partial Grotrian diagram constructed from the compilation of Martin et al. (1978) for this ion. A total of 117 even-parity and 243 odd-parity levels are included in the compilation. The substantial overlap of low configurations leads to extensive configuration interaction and makes definitive assignments quite difficult for many levels. The lack of level assignments causes only minor difficulties in experimental work on branching fractions and transition probabilities since one cannot guess the strongest branches from an upper level. However, the lack of level assignments makes ab initio theoretical determination of transition probability data very difficult.

Configuration and term assignments are firm for the lowest 26 levels of the 117 known even-parity levels including: 12 levels of the $4f^{12}(^3H)6s_{1/2}$ and $4f^{12}(^3F)6s_{1/2}$ subconfigurations, 10 levels of the $4f^{12}(^3H_6)5d_{3/2}$ and $4f^{12}(^3H_6)5d_{5/2}$ subconfigurations, and four levels $4f^{12}(^3F_4)5d_{3/2}$ subconfigurations. Fortunately this list of low even-parity levels with firm assignments is nearly complete below ~20,000 $cm^{-1}$. Although there is a missing $4f^{12}(^1G)6s_{1/2}{}^2G$ term in the 15,000–20,000 $cm^{-1}$ range, the nearly complete list of even-parity levels <20,000 $cm^{-1}$ reduces concerns of possible strong branches to unobserved low even-parity levels affecting the accuracy of our branching fraction measurements from upper odd-parity levels. Above 20,000 $cm^{-1}$ there are numerous unobserved even-parity levels. Between 25,000 and 31,000 $cm^{-1}$ there are only nine levels assigned to the $4f^{12}(^3H)5d$ subconfiguration and these lack term assignments. Except for the nine levels of the

$4f^{11}(^3H_{15/2})6s6p(^3P)$ subconfiguration between 32,000 and 38,000 cm$^{-1}$, the remaining even-parity levels are either tentatively assigned to the $4f^{11}(^4I)5d6p$ subconfiguration or in most cases unassigned. A new analysis of Er II is underway (J. F. Wyart et al. 2008, in preparation).

The fraction of observed levels with assignments is somewhat lower for the 243 known odd-parity levels. Only the lowest odd-parity level at 6825 cm$^{-1}$ and two higher levels have firm term assignments. These three levels are part of the low $^4I$ term of $4f^{11}6s^2$ configuration. Another 28 levels starting from 10,667 cm$^{-1}$ have firm assignments to the $4f^{11}(^4I)5d6s$ subconfiguration, and 7 have tentative assignments to this subconfiguration. These 38 levels are the lower levels of strong branches from the upper even-parity levels included in our branching fraction study. There are 10 additional levels ranging from 25,000 to 34,000 cm$^{-1}$ with tentative term and configuration assignments to the $4f^{12}6p$ configuration. All other odd-parity levels lack both term and configuration assignments. The ongoing reanalysis of Er II indicates that the lowest unobserved odd-parity level is just under 20,000 cm$^{-1}$ (J. F. Wyart et al. 2008, in preparation). There are quite a number of unobserved odd-parity levels in the 20,000–30,000 cm$^{-1}$ range. These levels, like many of the upper odd-parity levels included in our branching fraction study, are mixtures of states from $4f^{12}6p$, $4f^{11}6s^2$, $4f^{11}5d6s$, and $4f^{11}5d^2$ configurations.

The crucial issue in this review of assignments for low Er II levels is whether or not there are significant branches from upper levels in this study to unobserved lower levels. Although many previously unobserved levels have been located in the ongoing reanalysis of Er II (J. F. Wyart et al. 2008, in preparation), these levels are very weakly connected to upper levels of this study with one exception. We return to the issue of unobserved levels after discussing our branching fraction measurements.

### 2.2. Er II *Branching Fraction Analysis and Relative Radiometric Calibration*

As in earlier studies, our experimental branching fractions are based on a large set of FTS data including spectra of lamps at high currents to reveal very weak branches to known levels, good IR spectra to reveal any significant IR branches to known levels, and low current spectra in which dominant branches are optically thin covering the UV to near-IR. Table 1 is a list of the 15 FTS spectra used in our branching fraction study. All were recorded using the National Solar Observatory 1.0 m FTS on Kitt Peak. Some of these spectra (numbers 1–6, 12–15) were recorded by other guest observers in the 1980s, and others (7–11) were recorded during our 2000 February and 2002 February observing runs. All 15 raw spectra are available from the electronic archives of the National Solar Observatory.[7]

The establishment of an accurate relative radiometric calibration or efficiency is critical to a branching fraction experiment. As indicated in Table 1, we made use of both standard lamp calibrations and Ar I and Ar II line calibrations in this Er II study. Tungsten (W) filament standard lamps are particularly useful near the Si detector cutoff in the 10,000–9000 cm$^{-1}$ range, where the FTS sensitivity is changing rapidly as a function of wavenumber, and near the dip in sensitivity at 12,500 cm$^{-1}$ from the aluminum coated optics. Tungsten lamps are not bright enough to be useful for FTS calibrations in the UV region, and UV branches typically dominate the decay of levels studied using our lifetime experiment. In general one must be careful when using continuum lamps to calibrate the FTS over wide spectral ranges, because the "ghost" of a continuum is a continuum. The Ar I and Ar II line technique, which is internal to the hollow cathode discharge (HCD) Er/Ar lamp spectra, is still our preferred calibration technique. It captures the wavelength-dependent response of detectors, spectrometer optics, lamp windows, and any other components in the light path or any reflections that contribute to the detected signal (such as due to light reflecting off the back of the hollow cathode). This calibration technique is based on a comparison of well-known branching ratios for sets of Ar I and Ar II lines widely separated in wavelength, to the intensities measured for the same lines. Sets of Ar I and Ar II lines have been established for this purpose in the range of 4300–35,000 cm$^{-1}$ by Adams & Whaling (1981), Danzmann & Kock (1982), Hashiguchi & Hasikuni (1985), and Whaling et al. (1993). One of our best Er/Ar HCD spectra from 2002, and the Er/Ar HCD spectra from 1987 and 1988, were calibrated with both W standard lamp spectra recorded shortly before, or after, the HCD lamp spectra and using the Ar I and Ar II line technique. The Er/Ne spectra from 1987 and 1988 could only be calibrated using W standard lamp. The older W lamp is a strip lamp calibrated as a spectral radiance (W m$^{-2}$ sr$^{-1}$ nm$^{-1}$) standard, and the newer is a tungsten-quartz-halogen lamp calibrated as a spectral irradiance (W m$^{-2}$ nm$^{-1}$ at a specified distance) standard. Neither of these W filament lamps is hot or bright enough to yield a reliable UV calibration, but they are useful in the visible and near-IR for interpolation and as a redundant calibration.

All possible transition wavenumbers between known energy levels of Er II satisfying both the parity change and $\Delta J = -1, 0$, or 1 selection rules were computed and used during analysis of FTS data. Energy levels from Martin et al. (1978) were used to determine possible transition wavenumbers. Levels from Martin et al. (1978) are available in electronic form from Martin et al. (2000).[8] Systematic errors from missing branches to known lower levels are negligible in our work, because we were able to make at least rough measurements on ultraviolet through IR lines with branching fractions of 0.001 or smaller. This is illustrated in Table 2, which lists our branching fractions for the odd-parity upper level at 28361.386 cm$^{-1}$. For this level we were able to measure and report a very weak, 0.00040, branching fraction. Figures 2 and 3 show some Er II line profiles from this upper level. Figure 2 is the shortest wavelength, second strongest transition at 3524.905 Å (branching fraction 0.389). Figure 3 is the second longest wavelength transition at 15458.105 Å (branching fraction 0.00122). Given the large wavelength separation of these two lines, it should not be surprising that the data in Figures 2 and 3 are from different spectra. Isotopic structure is clearly visible in the IR line of Figure 3. The triplet pattern is due to the even (nuclear spin $I = 0$) isotopes $^{166}$Er (abundance 33.61%), $^{168}$Er (abundance 26.78%), and $^{170}$Er (abundance 14.93%) (Rosman & Taylor 1998). Hyperfine structure "smears out" the transition of the other abundant Er isotope, which is the odd ($I = 7/2$) isotope $^{167}$Er (abundance 22.93%) and individual hyperfine components from this odd isotope are difficult to detect in our spectra. The two lightest isotopes, $^{164}$Er (abundance 1.61%) and $^{162}$Er (abundance 0.14%), have such low abundances that they are not detectable in our spectra. Isotopic splittings are somewhat larger in the IR than in the UV for lines studied, but one should keep in mind that the FTS data of Figure 3 has higher spectral resolution than that of Figure 2. The IR lines with relatively large isotope shifts are very weak and have such large excitation potentials that we see no hope of detecting the lines in astrophysical spectra for the foreseeable future.

[7] Available at http://nsokp.nso.edu.

[8] Available at http://physics.nist.gov/PhysRefData/ASD/index.html.

TABLE 1

FOURIER TRANSFORM SPECTRA OF Er LAMPS USED IN THIS STUDY

| Index | Date | Serial Number | Lamp Type[a] | Buffer Gas | Lamp Current (mA) | Wavenumber Range ($cm^{-1}$) | Limit of Resolution ($cm^{-1}$) | Co-adds | Beam Splitter | Filter | Detector[b] | Calibration[c] |
|---|---|---|---|---|---|---|---|---|---|---|---|---|
| 1..... | 1988 Nov 10 | 3 | Custom HCD | Ar | 500 | 7346–42640 | 0.055 | 8 | UV | ... | SB Si Diode | Ar I & II W Strip Lamp |
| 2..... | 1988 Nov 11 | 4 | Custom HCD | Ar | 500 | 13437–42640 | 0.055 | 8 | UV | $CuSO_4$ | SB Si Diode | Ar I & II W Strip Lamp |
| 3..... | 1987 Jan 13 | 2 | Custom HCD | Ar | 500 | 8218–26091 | 0.050 | 8 | Vis | ... | SB Si Diode | Ar I & II W Strip Lamp |
| 4..... | 1987 Jan 13 | 1 | Custom HCD | Ar | 500 | 8218–26091 | 0.100 | 12 | Vis | ... | SB Si Diode | Ar I & II W Strip Lamp |
| 5..... | 1987 Jan 14 | 8 | Custom HCD | Ar | 300 | 8218–26091 | 0.050 | 1 | Vis | ... | SB Si Diode | Ar I & II W Strip Lamp |
| 6..... | 1987 Jan 13 | 5 | Custom HCD | Ar | 500 | 3488 –15077 | 0.029 | 8 | Vis | ... | InSb | Ar I & II W Strip Lamp |
| 7..... | 2000 Feb 28 | 32 | Commercial HCD | Ar | 26.5 | 7929–34998 | 0.053 | 59 | UV | ... | SB Si Diode | Ar I & II |
| 8..... | 2002 Feb 26 | 10 | Commercial HCD | Ar | 27 | 7929–34998 | 0.050 | 50 | UV | ... | SB Si Diode | Ar I & II WQH Lamp |
| 9..... | 2000 Feb 28 | 27 | Commercial HCD | Ar | 26.5 | 7929–34998 | 0.053 | 16 | UV | ... | SB Si Diode | Ar I & II |
| 10..... | 2000 Feb 28 | 26 | Commercial HCD | Ar | 23 | 7929–34998 | 0.053 | 4 | UV | ... | SB Si Diode | Ar I & II |
| 11..... | 2000 Feb 28 | 28 | Commercial HCD | Ar | 17 | 7929–34998 | 0.053 | 4 | UV | ... | SB Si Diode | Ar I & II |
| 12..... | 1988 Nov 10 | 1 | Custom HCD | Ne | 300 | 7346–42640 | 0.055 | 8 | UV | ... | SB Si Diode | W Strip Lamp |
| 13..... | 1988 Nov 10 | 2 | Custom HCD | Ne | 300 | 13437–42640 | 0.055 | 8 | UV | ... | SB Si Diode | W Strip Lamp |
| 14..... | 1987 Jan 13 | 3 | Custom HCD | Ne | 300 | 8218–26091 | 0.050 | 8 | Vis | ... | SB Si Diode | W Strip Lamp |
| 15..... | 1987 Jan 13 | 4 | Custom HCD | Ne | 310 | 3488–15017 | 0.029 | 8 | UV | ... | InSb | W Strip Lamp |

NOTE.—All spectra were recorded using the 1.0 m FTS on the McMath telescope at the National Solar Observatory, Kitt Peak, AZ.

[a] Lamp types include commercially available small sealed hollow cathode discharge (HCD) lamps typically used in atomic absorption spectrophotometers and a custom water-cooled HCD lamp.

[b] Detectors types include the Super Blue (SB) Si photodiode.

[c] Relative radiometric calibrations were based on selected sets of Ar I and Ar II lines, on a tungsten-quartz-halogen (WQH) lamp calibrated as a secondary irradiance standard, and on a tungsten (W) strip lamp calibrated as a secondary radiance standard.

TABLE 2

BRANCHING FRACTIONS FOR AN ODD-PARITY UPPER LEVEL OF Er II ORGANIZED BY INCREASING WAVELENGTH IN AIR, $\lambda_{air}$

| Wavenumber ($cm^{-1}$) | $\lambda_{air}$ (Å) | $E_{upper}$ ($cm^{-1}$) | $J_{upp}$ | $E_{lower}$ ($cm^{-1}$) | $J_{low}$ | Branching Fraction |
|---|---|---|---|---|---|---|
| 28361.39..... | 3524.91 | 28361.39 | 5.5 | 0.00 | 6.5 | 0.389 ± 0.004 |
| 27920.95..... | 3580.52 | 28361.39 | 5.5 | 440.43 | 5.5 | 0.569 ± 0.006 |
| 23228.78..... | 4303.79 | 28361.39 | 5.5 | 5132.61 | 4.5 | 0.0100 ± 0.0009 |
| 21166.03..... | 4723.23 | 28361.39 | 5.5 | 7195.35 | 4.5 | 0.0083 ± 0.0007 |
| 11808.51..... | 8466.14 | 28361.39 | 5.5 | 16552.87 | 4.5 | 0.0098 ± 0.0018 |
| 9472.28..... | 10554.22 | 28361.39 | 5.5 | 18889.10 | 5.5 | 0.0034 ± 0.0007 |
| 7633.34..... | 13096.85 | 28361.39 | 5.5 | 20728.05 | 6.5 | 0.00040 ± 0.00010 |
| 6663.53..... | 15002.95 | 28361.39 | 5.5 | 21697.85 | 5.5 | 0.0029 ± 0.0007 |
| 6467.33..... | 15458.11 | 28361.39 | 5.5 | 21894.06 | 4.5 | 0.00122 ± 0.00029 |
| 6220.03..... | 16072.70 | 28361.39 | 5.5 | 22141.35 | 6.5 | 0.0033 ± 0.0008 |

Branching fraction measurements were attempted on lines from all 80 levels of the lifetime experiment by Stockett et al. (2007), and were completed for lines from 7 even-parity and 63 odd-parity upper levels. The levels for which branching fractions could not be completed had a strong branch beyond the UV limit of our spectra, or had a strong branch that was severely blended. Typically an odd-parity upper level, depending on its $J$ value, has about 20 possible transitions to known lower levels, and an even-parity upper level has about 60 possible transitions to known lower levels. More than 20,000 possible spectral line observations were studied during the analysis of 15 different Er/Ar and Er/Ne spectra. We set integration limits and occasionally nonzero baselines "interactively" during analysis of the FTS spectra. An occasional nonzero baseline is needed when a weak line is located on a line wing of a much stronger line. The same numerical integration routine was used to determine the uncalibrated intensities of Er II lines and selected Ar I and Ar II lines used to establish a relative radiometric calibration of the spectra. A simple numerical integration technique was used in this and most of our other RE studies because of weakly resolved or unresolved hyperfine and isotopic structure. More sophisticated profile fitting is used only when the line subcomponent structure is either fully resolved in the FTS data or known from independent measurements.

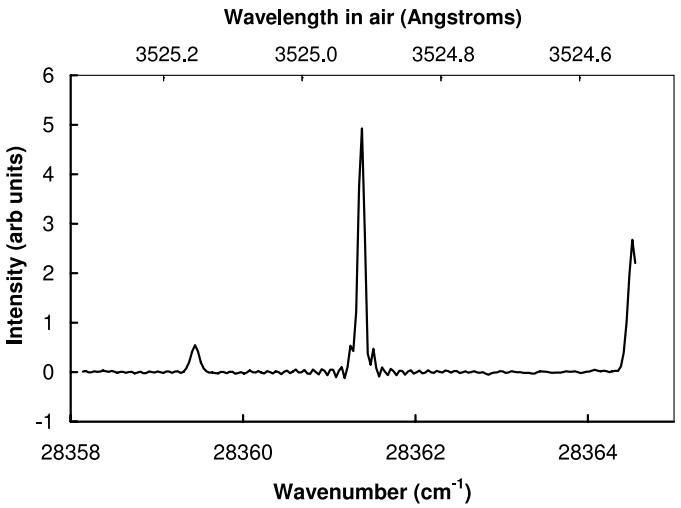


FIG. 2.—FTS data from spectrum 7 of Table 1. The Er II line near the center of the plot is from the odd-parity upper level at 28361.386 $cm^{-1}$ to the even-parity ground level at 0.000 $cm^{-1}$. This UV line at 3524.913 Å is the second strongest branch from the upper level with a branching fraction of 0.389. There are Er I lines visible at a somewhat lower wavenumber and at a higher wavenumber near the left edge of the plot. Ringing from the apodization of the interferogram is visible as well as some weak isotopic structure near the base of the line.

### 2.3. *Branching Fraction Uncertainties*

The procedure for determining branching fraction uncertainties was described in detail by Wickliffe et al. (2000). Branching fractions from a given upper level are defined to sum to unity, thus a dominant line from an upper level has small branching fraction uncertainty almost by definition. Branching fractions for weaker lines near the dominant line(s) tend to have uncertainties limited by their S/N ratios. Systematic uncertainties in the radiometric calibration are typically the most serious source of uncertainty for widely separated lines from a common upper level. We used a formula for estimating this systematic uncertainty that was presented and tested extensively by Wickliffe et al. (2000). The spectra of the high-current custom HCD lamps enabled us to connect the stronger visible and near-IR branches to quite weak branches in the same spectral range. Uncertainties grew to some extent from piecing together branching ratios from so many spectra, but such effects have been included in the uncertainties on branching fractions of the weak visible and near-IR lines. In the final analysis, the branching fraction uncertainties are primarily systematic. Redundant measurements with independent radiometric calibrations help in the assessment of systematic uncertainties. Redundant measurements from spectra with different discharge conditions also make it easier to spot blended lines and optically thick lines. Many of the strong lines in the UV and visible were optically thick in the spectra from the custom

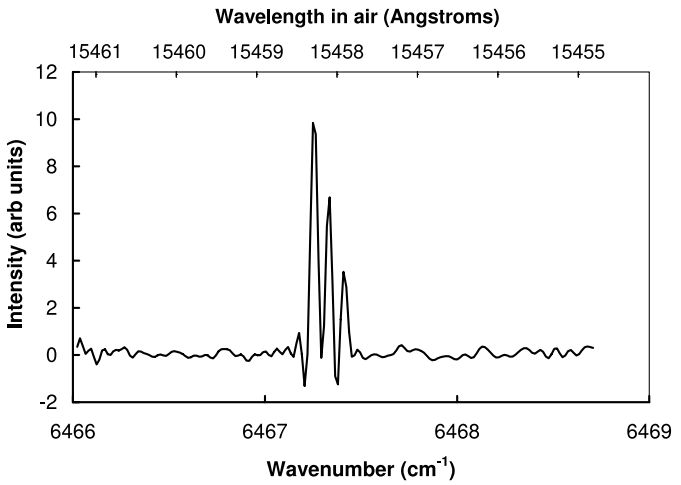


FIG. 3.—FTS data from spectrum 6 of Table 1. The Er II line near the center of the plot is from the odd-parity upper level at 28361.386 $cm^{-1}$ to the even-parity lower level at 21894.055 $cm^{-1}$. This IR line at 15458.105 Å is the second weakest branch reported from the upper level with a branching fraction of 0.00122. The triplet structure is from the dominant even (nuclear spin $I = 0$) isotopes.

HCD lamp operating at high current. These data were discarded during review of the branching ratio data before combining data from the various spectra to determine our final branching fractions.

As mentioned in § 2.1, one of the more troubling systematic uncertainties is from possible branches to unobserved lower levels. We have checked for branches from upper levels in this study to previously unobserved lower levels using both an experimental search to tentatively identified lower levels, and using results from a parametric fit to the energy levels. With only one exception, the upper levels of this study are very weakly connected to the unobserved lower levels. On the basis of the reanalysis of Er II to date, only the highest upper level of this study, the even-parity level at 46757.780 $cm^{-1}$, is likely to have significant branches to unobserved odd-parity lower levels (J. F. Wyart et al. 2008, in preparation). Transition probabilities from this upper level have been reduced by 7.7% (∼0.03 dex) to correct for the branches to unobserved lower levels. This correction introduces some additional systematic uncertainty for the four lines from this upper level included in our study. The reanalysis indicates that the odd-parity upper level at 33307.365 $cm^{-1}$ has $J = 3.5$ (7/2 in standard notation) instead of 4.5 (9/2) as given in the NIST tables (Martin et al. 1978).[9] The Landé $g$-factor supports this change. Careful inspection of all spectra in this study revealed some weak lines from this upper level to $J = 2.5$ (5/2) lower level and not a hint of a transition to a lower level with $J = 5.5$ (11/2). We therefore use the modified $J = 3.5$ (7/2) for the level at 33307.365 $cm^{-1}$ and note that this change does not affect our Einstein $A$-coefficients from this upper level, but does affect the log ($gf$) values from this upper level. The reanalysis also indicates that the $J = 4.5$ (9/2) odd-parity level at 33129.912 $cm^{-1}$ is not real. Only a single emission line at 3570.75 Å from this upper level was detected in our branching fraction study, and this level does not fit in the parametric study of Er II (J. F. Wyart et al. 2008, in preparation). The lifetime of 4.7 ns reported by Stockett et al. (2007) is correct for laser excitation at 3570.75 Å, but no transition probabilities can be reported until the $J$ and actual energy of the upper level is established.

### 2.4. Er II *Atomic Transition Probabilities*

Branching fractions from the FTS spectra were combined with the radiative lifetime measurements (Stockett et al. 2007) to determine absolute transition probabilities for 418 lines of Er II in Table 3. Air wavelengths in Table 3 were computed from energy levels (Martin et al. 1978) using the standard index of air (Edlén 1953). Parities are included in Table 3 using "ev" and "od" notation that is compatible with our main machine-readable table of transition probabilities.

Transition probabilities for the very weakest lines (branching fractions ∼ 0.001 or weaker) that were observed with poor S/N ratios and for a few blended lines are not included in Table 3, but these lines are included in the branching fraction normalization. The effect of the problem lines becomes apparent if one sums all transition probabilities in Table 3 from a chosen upper level and compares the sum to the inverse of the upper level lifetime from Stockett et al. (2007). Typically the sum of the Table 3 transition probabilities is between 95% and 100% of the inverse lifetime. Although there is significant fractional uncertainty in the branching fractions for these problem lines, this does not have much effect on the uncertainty of the stronger lines that were kept in Table 3. Branching fraction uncertainties are combined in quadrature with lifetime uncertainties to determine the transition probability uncertainties in Table 3.

There are only a few comparisons that can be made between our transition probability data and other similar data. The most interesting comparison is to the experimental work of Musiol & Labuz (1983) shown in Figure 4. The discordant points of Figure 4 may be, in some cases, due to incorrect line identifications from the lower resolving power achieved in the earlier grating spectrometer measurements by Musiol and Labuz. In complex rare-earth spectra, the resolution and absolute wavenumber accuracy of a FTS is extremely important. Line broadening and blending could also have been a problem in the experiments by Musiol and Labuz because they used a high-pressure (LTE) arc plasma. Lines from our low-pressure HCD lamps are primarily Doppler broadened in most cases. Although the comparison to Musiol & Labuz (1983) is not as favorable as one might hope, it is better than the comparisons to theoretical results in Figures 5 and 6. Figures 5 and 6 are, respectively, comparisons of our results against relativistic Hartree Fock calculations (Xu et al. 2003) and semi-empirical results.[10] It is important to recall that the very comprehensive Kurucz database was originally intended for opacity calculations, and not for precise spectroscopic research. (It should also be noted that some of the Kurucz data are from Musiol & Labuz 1983.) Calculations of transition probabilities in Er II are indeed a very difficult theoretical undertaking. We note that the reanalysis of Er II is yielding encouraging results. Theoretical branching fractions are in good agreement with experimental branching fractions for all of the even-parity upper levels in this study, and for about half of the odd-parity upper levels. In the next sections we apply our new laboratory results in Er abundance determinations.

## 3. SOLAR AND STELLAR ERBIUM ABUNDANCES

The new transition probabilities have been applied to Er II lines in the solar photosphere and five very metal poor ($[Fe/H] < -2$)[11] stars that have large overabundances of the rare-earth elements. Our abundance study followed the methods used for Hf II by Lawler et al. (2007) and previous papers in this series. Erbium has been less well studied in solar/stellar spectra than have many other rare-earth ions, due to a lack of extensive previous lab investigations and to a paucity of transitions in spectral regions convenient for ground-based high-resolution spectroscopy. Anecdotal evidence to support this suggestion comes from the classic Moore et al. (1966) solar line compendium. Those authors could identify only two Er II transitions (at 3896.2 and 3903.3 Å), in contrast with the large number they identified for many other rare-earth ions (e.g., 146 Sm II and 72 Gd II lines). Identification of a suitable set of Er II lines was therefore as important as the subsequent abundance analysis.

### 3.1. *Line Selection*

We have accurate transition probabilities for 418 Er II lines, but only a small minority of these can be employed to determine Er abundances in the Sun and our chosen metal-poor stars. This is because all strong Er II lines occur only in the near-UV spectral domain, $\lambda < 4000$ Å. As discussed by Lawler et al. (2007 and references therein), to first approximation the relative strengths of weak-to-moderate lines within one species depend directly on their transition probabilities modified by the Boltzmann excitation

[9] Redundant decimal notation and standard fractional notation for $J$ values are included in the text, but our tables use only decimal notation required for the main machine readable table of transition probabilities.

[10] See linelist at http://kurucz.harvard.edu.

[11] We adopt standard stellar spectroscopic notations that for elements A and B, $[A/B] = \log(N_A/N_B)_{star} - \log(N_A/N_B)_{Sun}$, for abundances relative to solar, and $\log \varepsilon(A) = \log(N_A/N_H) + 12.0$, for absolute abundances.

TABLE 3

ATOMIC TRANSITION PROBABILITIES FOR Er II ORGANIZED BY INCREASING WAVELENGTH IN AIR, $\lambda_{air}$

| $\lambda_{air}$ (Å) | $E_{upper}$ ($cm^{-1}$) | Parity | $J_{upp}$ | $E_{lower}$ ($cm^{-1}$) | Parity | $J_{low}$ | $A$-value ($10^6$ $s^{-1}$) | log ($gf$) |
|---|---|---|---|---|---|---|---|---|
| 2892.398 | 34563.257 | od | 5.5 | 0.000 | ev | 6.5 | 0.26 ± 0.04 | −2.41 |
| 2904.468 | 41244.400 | ev | 8.5 | 6824.774 | od | 7.5 | 93 ± 5 | 0.33 |
| 2910.362 | 41174.705 | ev | 7.5 | 6824.774 | od | 7.5 | 204 ± 11 | 0.62 |
| 2911.067 | 34341.611 | od | 5.5 | 0.000 | ev | 6.5 | 1.12 ± 0.18 | −1.77 |
| 2920.240 | 34674.173 | od | 4.5 | 440.434 | ev | 5.5 | 1.56 ± 0.16 | −1.70 |
| 2929.733 | 34563.257 | od | 5.5 | 440.434 | ev | 5.5 | 2.49 ± 0.28 | −1.41 |
| 2941.329 | 33988.301 | od | 5.5 | 0.000 | ev | 6.5 | 0.58 ± 0.07 | −2.05 |
| 2944.065 | 34397.143 | od | 4.5 | 440.434 | ev | 5.5 | 2.1 ± 0.3 | −1.57 |
| 2945.280 | 46757.780 | ev | 9.5 | 12815.068 | od | 9.5 | 46.9 ± 2.9 | 0.09 |
| 2964.520 | 40547.199 | ev | 8.5 | 6824.774 | od | 7.5 | 159 ± 8 | 0.58 |
| 2968.761 | 33674.250 | od | 6.5 | 0.000 | ev | 6.5 | 9.5 ± 0.5 | −0.75 |
| 2970.059 | 33659.536 | od | 5.5 | 0.000 | ev | 6.5 | 1.73 ± 0.23 | −1.56 |
| 2972.275 | 34074.875 | od | 4.5 | 440.434 | ev | 5.5 | 3.36 ± 0.25 | −1.35 |
| 2979.946 | 33988.301 | od | 5.5 | 440.434 | ev | 5.5 | 1.03 ± 0.13 | −1.79 |
| 3002.406 | 40121.685 | ev | 6.5 | 6824.774 | od | 7.5 | 130 ± 7 | 0.39 |
| 3003.832 | 33721.545 | od | 5.5 | 440.434 | ev | 5.5 | 1.76 ± 0.12 | −1.54 |
| 3008.107 | 33674.250 | od | 6.5 | 440.434 | ev | 5.5 | 0.322 ± 0.027 | −2.21 |
| 3009.439 | 33659.536 | od | 5.5 | 440.434 | ev | 5.5 | 0.44 ± 0.05 | −2.14 |
| 3012.472 | 46757.780 | ev | 9.5 | 13572.118 | od | 10.5 | 47 ± 3 | 0.11 |
| 3019.763 | 33105.534 | od | 5.5 | 0.000 | ev | 6.5 | 1.74 ± 0.17 | −1.54 |
| 3025.919 | 46757.780 | ev | 9.5 | 13719.584 | od | 8.5 | 36.4 ± 2.1 | 0.00 |
| 3028.275 | 33012.493 | od | 6.5 | 0.000 | ev | 6.5 | 4.95 ± 0.25 | −1.02 |
| 3031.309 | 39804.224 | ev | 7.5 | 6824.774 | od | 7.5 | 26.3 ± 2.3 | −0.24 |
| 3046.871 | 32811.006 | od | 5.5 | 0.000 | ev | 6.5 | 0.27 ± 0.05 | −2.34 |
| 3064.830 | 32618.753 | od | 5.5 | 0.000 | ev | 6.5 | 0.75 ± 0.08 | −1.90 |
| 3066.221 | 37736.569 | od | 4.5 | 5132.608 | ev | 4.5 | 12.8 ± 1.2 | −0.74 |
| 3069.224 | 33012.493 | od | 6.5 | 440.434 | ev | 5.5 | 2.09 ± 0.12 | −1.38 |
| 3073.344 | 32528.401 | od | 6.5 | 0.000 | ev | 6.5 | 12.4 ± 0.6 | −0.61 |
| 3080.206 | 32896.371 | od | 4.5 | 440.434 | ev | 5.5 | 0.52 ± 0.07 | −2.13 |
| 3091.929 | 37736.569 | od | 4.5 | 5403.688 | ev | 3.5 | 2.62 ± 0.24 | −1.43 |
| 3094.497 | 37438.656 | od | 4.5 | 5132.608 | ev | 4.5 | 0.59 ± 0.10 | −2.07 |
| 3106.781 | 32618.753 | od | 5.5 | 440.434 | ev | 5.5 | 3.68 ± 0.27 | −1.19 |
| 3113.537 | 46757.780 | ev | 9.5 | 14649.277 | od | 9.5 | 73 ± 4 | 0.33 |
| 3115.529 | 32528.401 | od | 6.5 | 440.434 | ev | 5.5 | 2.77 ± 0.18 | −1.25 |
| 3116.948 | 32073.360 | od | 5.5 | 0.000 | ev | 6.5 | 3.48 ± 0.18 | −1.22 |
| 3122.722 | 37146.674 | od | 5.5 | 5132.608 | ev | 4.5 | 3.60 ± 0.26 | −1.20 |
| 3141.095 | 32267.246 | od | 4.5 | 440.434 | ev | 5.5 | 4.4 ± 0.3 | −1.19 |
| 3143.634 | 31801.102 | od | 5.5 | 0.000 | ev | 6.5 | 1.84 ± 0.10 | −1.49 |
| 3160.348 | 32073.360 | od | 5.5 | 440.434 | ev | 5.5 | 3.94 ± 0.21 | −1.15 |
| 3160.786 | 36761.150 | od | 4.5 | 5132.608 | ev | 4.5 | 2.28 ± 0.19 | −1.47 |
| 3181.920 | 31418.481 | od | 6.5 | 0.000 | ev | 6.5 | 17.5 ± 0.9 | −0.43 |
| 3183.418 | 31844.124 | od | 4.5 | 440.434 | ev | 5.5 | 12.5 ± 0.8 | −0.72 |
| 3185.247 | 31385.667 | od | 5.5 | 0.000 | ev | 6.5 | 5.8 ± 0.3 | −0.98 |
| 3187.786 | 31801.102 | od | 5.5 | 440.434 | ev | 5.5 | 3.07 ± 0.16 | −1.25 |
| 3188.112 | 36761.150 | od | 4.5 | 5403.688 | ev | 3.5 | 1.11 ± 0.09 | −1.77 |
| 3227.161 | 31418.481 | od | 6.5 | 440.434 | ev | 5.5 | 3.04 ± 0.17 | −1.18 |
| 3230.583 | 31385.667 | od | 5.5 | 440.434 | ev | 5.5 | 92 ± 5 | 0.24 |
| 3237.977 | 36007.182 | od | 4.5 | 5132.608 | ev | 4.5 | 19.1 ± 1.0 | −0.52 |
| 3246.344 | 35927.604 | od | 3.5 | 5132.608 | ev | 4.5 | 0.45 ± 0.06 | −2.25 |
| 3257.734 | 35819.939 | od | 3.5 | 5132.608 | ev | 4.5 | 3.01 ± 0.19 | −1.42 |
| 3264.781 | 30621.102 | od | 6.5 | 0.000 | ev | 6.5 | 69 ± 3 | 0.19 |
| 3266.659 | 36007.182 | od | 4.5 | 5403.688 | ev | 3.5 | 6.1 ± 0.4 | −1.01 |
| 3268.427 | 37736.569 | od | 4.5 | 7149.630 | ev | 5.5 | 3.9 ± 0.5 | −1.21 |
| 3273.321 | 37736.569 | od | 4.5 | 7195.355 | ev | 4.5 | 9.2 ± 0.7 | −0.83 |
| 3275.176 | 35927.604 | od | 3.5 | 5403.688 | ev | 3.5 | 1.06 ± 0.15 | −1.87 |
| 3280.217 | 30917.436 | od | 4.5 | 440.434 | ev | 5.5 | 16.2 ± 0.8 | −0.58 |
| 3286.769 | 35819.939 | od | 3.5 | 5403.688 | ev | 3.5 | 35.9 ± 1.8 | −0.33 |
| 3300.575 | 37438.656 | od | 4.5 | 7149.630 | ev | 5.5 | 2.81 ± 0.25 | −1.34 |
| 3305.566 | 37438.656 | od | 4.5 | 7195.355 | ev | 4.5 | 32.1 ± 1.7 | −0.28 |
| 3312.426 | 30621.102 | od | 6.5 | 440.434 | ev | 5.5 | 40.9 ± 2.1 | −0.03 |
| 3314.944 | 30157.742 | od | 5.5 | 0.000 | ev | 6.5 | 1.09 ± 0.06 | −1.66 |
| 3318.774 | 30122.939 | od | 5.5 | 0.000 | ev | 6.5 | 1.80 ± 0.12 | −1.45 |
| 3323.194 | 35215.487 | od | 5.5 | 5132.608 | ev | 4.5 | 34.3 ± 1.9 | −0.17 |
| 3332.703 | 37146.674 | od | 5.5 | 7149.630 | ev | 5.5 | 59 ± 3 | 0.07 |

TABLE 3—*Continued*

| $\lambda_{air}$ (Å) | $E_{upper}$ ($cm^{-1}$) | Parity | $J_{upp}$ | $E_{lower}$ ($cm^{-1}$) | Parity | $J_{low}$ | $A$-value ($10^6$ $s^{-1}$) | log ($gf$) |
|---|---|---|---|---|---|---|---|---|
| 3337.791..... | 37146.674 | od | 5.5 | 7195.355 | ev | 4.5 | 24.6 ± 1.3 | −0.31 |
| 3339.586..... | 41244.400 | ev | 8.5 | 11309.180 | od | 7.5 | 2.36 ± 0.26 | −1.15 |
| 3340.026..... | 35063.892 | od | 4.5 | 5132.608 | ev | 4.5 | 13.6 ± 0.7 | −0.64 |
| 3346.034..... | 30317.974 | od | 4.5 | 440.434 | ev | 5.5 | 25.6 ± 1.3 | −0.37 |
| 3348.141..... | 29858.739 | od | 5.5 | 0.000 | ev | 6.5 | 2.71 ± 0.14 | −1.26 |
| 3358.153..... | 34902.323 | od | 3.5 | 5132.608 | ev | 4.5 | 9.9 ± 0.5 | −0.88 |
| 3364.076..... | 30157.742 | od | 5.5 | 440.434 | ev | 5.5 | 18.5 ± 0.9 | −0.42 |
| 3368.020..... | 30122.939 | od | 5.5 | 440.434 | ev | 5.5 | 18.8 ± 0.9 | −0.42 |
| 3370.553..... | 35063.892 | od | 4.5 | 5403.688 | ev | 3.5 | 18.5 ± 0.9 | −0.50 |
| 3372.752..... | 29640.863 | od | 7.5 | 0.000 | ev | 6.5 | 145 ± 7 | 0.60 |
| 3374.170..... | 29628.405 | od | 6.5 | 0.000 | ev | 6.5 | 15.2 ± 0.8 | −0.44 |
| 3376.094..... | 36761.150 | od | 4.5 | 7149.630 | ev | 5.5 | 9.5 ± 0.5 | −0.79 |
| 3378.757..... | 30028.618 | od | 4.5 | 440.434 | ev | 5.5 | 0.48 ± 0.04 | −2.09 |
| 3381.316..... | 36761.150 | od | 4.5 | 7195.355 | ev | 4.5 | 34.1 ± 1.8 | −0.23 |
| 3384.089..... | 34674.173 | od | 4.5 | 5132.608 | ev | 4.5 | 2.71 ± 0.17 | −1.33 |
| 3389.014..... | 34902.323 | od | 3.5 | 5403.688 | ev | 3.5 | 0.92 ± 0.08 | −1.90 |
| 3389.739..... | 29492.329 | od | 5.5 | 0.000 | ev | 6.5 | 6.1 ± 0.3 | −0.90 |
| 3391.987..... | 29472.789 | od | 7.5 | 0.000 | ev | 6.5 | 28.3 ± 1.4 | −0.11 |
| 3394.093..... | 40121.685 | ev | 6.5 | 10667.186 | od | 6.5 | 11.8 ± 1.0 | −0.54 |
| 3396.843..... | 34563.257 | od | 5.5 | 5132.608 | ev | 4.5 | 11.1 ± 0.6 | −0.64 |
| 3398.269..... | 29858.739 | od | 5.5 | 440.434 | ev | 5.5 | 2.07 ± 0.10 | −1.37 |
| 3406.956..... | 29783.733 | od | 4.5 | 440.434 | ev | 5.5 | 1.23 ± 0.09 | −1.67 |
| 3416.126..... | 34397.143 | od | 4.5 | 5132.608 | ev | 4.5 | 2.65 ± 0.21 | −1.33 |
| 3422.620..... | 34341.611 | od | 5.5 | 5132.608 | ev | 4.5 | 1.00 ± 0.12 | −1.68 |
| 3425.087..... | 29628.405 | od | 6.5 | 440.434 | ev | 5.5 | 3.11 ± 0.16 | −1.12 |
| 3433.128..... | 29119.606 | od | 6.5 | 0.000 | ev | 6.5 | 2.10 ± 0.11 | −1.28 |
| 3439.723..... | 34196.388 | od | 4.5 | 5132.608 | ev | 4.5 | 0.58 ± 0.05 | −1.98 |
| 3441.130..... | 29492.329 | od | 5.5 | 440.434 | ev | 5.5 | 12.5 ± 0.6 | −0.58 |
| 3448.066..... | 34397.143 | od | 4.5 | 5403.688 | ev | 3.5 | 7.9 ± 0.5 | −0.85 |
| 3464.528..... | 33988.301 | od | 5.5 | 5132.608 | ev | 4.5 | 8.2 ± 0.5 | −0.75 |
| 3469.722..... | 40121.685 | ev | 6.5 | 11309.180 | od | 7.5 | 32.5 ± 2.3 | −0.09 |
| 3469.803..... | 36007.182 | od | 4.5 | 7195.355 | ev | 4.5 | 1.89 ± 0.17 | −1.47 |
| 3472.108..... | 34196.388 | od | 4.5 | 5403.688 | ev | 3.5 | 0.143 ± 0.016 | −2.59 |
| 3479.414..... | 35927.604 | od | 3.5 | 7195.355 | ev | 4.5 | 39.4 ± 2.0 | −0.24 |
| 3485.853..... | 29119.606 | od | 6.5 | 440.434 | ev | 5.5 | 8.6 ± 0.4 | −0.66 |
| 3486.824..... | 34074.875 | od | 4.5 | 5403.688 | ev | 3.5 | 12.1 ± 0.7 | −0.66 |
| 3492.501..... | 35819.939 | od | 3.5 | 7195.355 | ev | 4.5 | 7.4 ± 0.4 | −0.96 |
| 3496.856..... | 33721.545 | od | 5.5 | 5132.608 | ev | 4.5 | 11.1 ± 0.6 | −0.61 |
| 3499.103..... | 29011.015 | od | 4.5 | 440.434 | ev | 5.5 | 105 ± 5 | 0.29 |
| 3504.457..... | 33659.536 | od | 5.5 | 5132.608 | ev | 4.5 | 1.36 ± 0.11 | −1.52 |
| 3508.379..... | 39804.224 | ev | 7.5 | 11309.180 | od | 7.5 | 44.3 ± 2.4 | 0.12 |
| 3515.999..... | 33565.895 | od | 4.5 | 5132.608 | ev | 4.5 | 2.62 ± 0.15 | −1.31 |
| 3516.488..... | 41244.400 | ev | 8.5 | 12815.068 | od | 9.5 | 4.2 ± 0.4 | −0.86 |
| 3518.176..... | 39082.884 | ev | 6.5 | 10667.186 | od | 6.5 | 28.5 ± 1.5 | −0.13 |
| 3524.913..... | 28361.386 | od | 5.5 | 0.000 | ev | 6.5 | 7.2 ± 0.4 | −0.79 |
| 3543.017..... | 41244.400 | ev | 8.5 | 13027.927 | od | 8.5 | 20.7 ± 1.7 | −0.15 |
| 3548.263..... | 33307.365 | od | 3.5 | 5132.608 | ev | 4.5 | 12.9 ± 0.7 | −0.71 |
| 3549.844..... | 33565.895 | od | 4.5 | 5403.688 | ev | 3.5 | 27.2 ± 1.4 | −0.29 |
| 3551.790..... | 41174.705 | ev | 7.5 | 13027.927 | od | 8.5 | 11.9 ± 1.1 | −0.44 |
| 3553.203..... | 33539.273 | od | 3.5 | 5403.688 | ev | 3.5 | 12.0 ± 0.6 | −0.74 |
| 3559.894..... | 28082.701 | od | 6.5 | 0.000 | ev | 6.5 | 7.6 ± 0.4 | −0.69 |
| 3573.865..... | 33105.534 | od | 5.5 | 5132.608 | ev | 4.5 | 2.78 ± 0.17 | −1.19 |
| 3580.518..... | 28361.386 | od | 5.5 | 440.434 | ev | 5.5 | 10.5 ± 0.5 | −0.62 |
| 3581.376..... | 35063.892 | od | 4.5 | 7149.630 | ev | 5.5 | 1.89 ± 0.17 | −1.44 |
| 3583.748..... | 33028.394 | od | 4.5 | 5132.608 | ev | 4.5 | 0.49 ± 0.03 | −2.02 |
| 3587.252..... | 35063.892 | od | 4.5 | 7195.355 | ev | 4.5 | 2.50 ± 0.23 | −1.32 |
| 3599.501..... | 39082.884 | ev | 6.5 | 11309.180 | od | 7.5 | 52.2 ± 2.7 | 0.15 |
| 3600.790..... | 32896.371 | od | 4.5 | 5132.608 | ev | 4.5 | 2.09 ± 0.17 | −1.39 |
| 3604.707..... | 40121.685 | ev | 6.5 | 12388.090 | od | 5.5 | 19.9 ± 1.6 | −0.27 |
| 3604.897..... | 40547.199 | ev | 8.5 | 12815.068 | od | 9.5 | 42 ± 3 | 0.17 |
| 3608.171..... | 34902.323 | od | 3.5 | 7195.355 | ev | 4.5 | 3.39 ± 0.22 | −1.28 |
| 3611.896..... | 32811.006 | od | 5.5 | 5132.608 | ev | 4.5 | 0.079 ± 0.015 | −2.73 |
| 3616.566..... | 27642.658 | od | 5.5 | 0.000 | ev | 6.5 | 21.0 ± 1.1 | −0.31 |
| 3616.617..... | 28082.701 | od | 6.5 | 440.434 | ev | 5.5 | 3.43 ± 0.17 | −1.03 |
| 3618.916..... | 33028.394 | od | 4.5 | 5403.688 | ev | 3.5 | 16.2 ± 0.8 | −0.50 |

TABLE 3—*Continued*

| $\lambda_{air}$ (Å) | $E_{upper}$ ($cm^{-1}$) | Parity | $J_{upp}$ | $E_{lower}$ ($cm^{-1}$) | Parity | $J_{low}$ | $A$-value ($10^6$ $s^{-1}$) | log ($gf$) |
|---|---|---|---|---|---|---|---|---|
| 3632.050..... | 41244.400 | ev | 8.5 | 13719.584 | od | 8.5 | 20.6 ± 2.0 | −0.13 |
| 3632.086..... | 34674.173 | od | 4.5 | 7149.630 | ev | 5.5 | 12.7 ± 0.7 | −0.60 |
| 3632.781..... | 40547.199 | ev | 8.5 | 13027.927 | od | 8.5 | 12.1 ± 1.3 | −0.37 |
| 3633.536..... | 27513.555 | od | 6.5 | 0.000 | ev | 6.5 | 10.6 ± 0.5 | −0.53 |
| 3636.295..... | 32896.371 | od | 4.5 | 5403.688 | ev | 3.5 | 1.29 ± 0.09 | −1.59 |
| 3637.160..... | 32618.753 | od | 5.5 | 5132.608 | ev | 4.5 | 5.4 ± 0.3 | −0.89 |
| 3638.130..... | 34674.173 | od | 4.5 | 7195.355 | ev | 4.5 | 0.61 ± 0.04 | −1.92 |
| 3641.270..... | 41174.705 | ev | 7.5 | 13719.584 | od | 8.5 | 28.1 ± 2.9 | −0.05 |
| 3646.782..... | 34563.257 | od | 5.5 | 7149.630 | ev | 5.5 | 2.18 ± 0.12 | −1.28 |
| 3652.585..... | 32502.680 | od | 4.5 | 5132.608 | ev | 4.5 | 7.6 ± 0.4 | −0.82 |
| 3652.875..... | 34563.257 | od | 5.5 | 7195.355 | ev | 4.5 | 12.6 ± 0.7 | −0.52 |
| 3669.015..... | 34397.143 | od | 4.5 | 7149.630 | ev | 5.5 | 15.5 ± 0.8 | −0.50 |
| 3675.182..... | 34397.143 | od | 4.5 | 7195.355 | ev | 4.5 | 2.14 ± 0.12 | −1.36 |
| 3676.508..... | 34341.611 | od | 5.5 | 7149.630 | ev | 5.5 | 5.07 ± 0.27 | −0.91 |
| 3682.701..... | 34341.611 | od | 5.5 | 7195.355 | ev | 4.5 | 17.3 ± 0.9 | −0.38 |
| 3684.278..... | 32267.246 | od | 4.5 | 5132.608 | ev | 4.5 | 11.7 ± 0.6 | −0.62 |
| 3689.124..... | 32502.680 | od | 4.5 | 5403.688 | ev | 3.5 | 2.92 ± 0.16 | −1.22 |
| 3692.649..... | 27513.555 | od | 6.5 | 440.434 | ev | 5.5 | 67 ± 3 | 0.28 |
| 3694.308..... | 40121.685 | ev | 6.5 | 13060.715 | od | 6.5 | 7.6 ± 0.7 | −0.66 |
| 3696.249..... | 34196.388 | od | 4.5 | 7149.630 | ev | 5.5 | 15.9 ± 0.8 | −0.49 |
| 3702.508..... | 34196.388 | od | 4.5 | 7195.355 | ev | 4.5 | 1.61 ± 0.13 | −1.48 |
| 3707.638..... | 41244.400 | ev | 8.5 | 14280.723 | od | 7.5 | 46 ± 4 | 0.23 |
| 3710.793..... | 32073.360 | od | 5.5 | 5132.608 | ev | 4.5 | 0.78 ± 0.06 | −1.71 |
| 3717.247..... | 41174.705 | ev | 7.5 | 14280.723 | od | 7.5 | 8.7 ± 1.0 | −0.54 |
| 3719.247..... | 34074.875 | od | 4.5 | 7195.355 | ev | 4.5 | 2.20 ± 0.19 | −1.34 |
| 3721.457..... | 32267.246 | od | 4.5 | 5403.688 | ev | 3.5 | 2.14 ± 0.12 | −1.35 |
| 3724.358..... | 37736.569 | od | 4.5 | 10893.936 | ev | 3.5 | 14.1 ± 0.9 | −0.53 |
| 3724.907..... | 33988.301 | od | 5.5 | 7149.630 | ev | 5.5 | 6.9 ± 0.4 | −0.77 |
| 3729.524..... | 26805.448 | od | 5.5 | 0.000 | ev | 6.5 | 10.4 ± 0.5 | −0.59 |
| 3731.265..... | 33988.301 | od | 5.5 | 7195.355 | ev | 4.5 | 19.5 ± 1.0 | −0.31 |
| 3733.585..... | 39804.224 | ev | 7.5 | 13027.927 | od | 8.5 | 2.72 ± 0.25 | −1.04 |
| 3734.583..... | 26769.141 | od | 6.5 | 0.000 | ev | 6.5 | 1.64 ± 0.08 | −1.32 |
| 3738.162..... | 39804.224 | ev | 7.5 | 13060.715 | od | 6.5 | 46.8 ± 2.5 | 0.20 |
| 3742.640..... | 31844.124 | od | 4.5 | 5132.608 | ev | 4.5 | 20.6 ± 1.1 | −0.36 |
| 3744.984..... | 39082.884 | ev | 6.5 | 12388.090 | od | 5.5 | 18.6 ± 1.0 | −0.26 |
| 3745.106..... | 37736.569 | od | 4.5 | 11042.640 | ev | 4.5 | 15.2 ± 0.9 | −0.50 |
| 3748.677..... | 31801.102 | od | 5.5 | 5132.608 | ev | 4.5 | 0.61 ± 0.05 | −1.81 |
| 3762.303..... | 33721.545 | od | 5.5 | 7149.630 | ev | 5.5 | 0.87 ± 0.07 | −1.65 |
| 3766.157..... | 37438.656 | od | 4.5 | 10893.936 | ev | 3.5 | 20.8 ± 1.2 | −0.35 |
| 3768.788..... | 33721.545 | od | 5.5 | 7195.355 | ev | 4.5 | 2.43 ± 0.16 | −1.21 |
| 3769.011..... | 33674.250 | od | 6.5 | 7149.630 | ev | 5.5 | 0.42 ± 0.05 | −1.90 |
| 3771.103..... | 33659.536 | od | 5.5 | 7149.630 | ev | 5.5 | 7.0 ± 0.4 | −0.75 |
| 3777.619..... | 33659.536 | od | 5.5 | 7195.355 | ev | 4.5 | 5.01 ± 0.27 | −0.89 |
| 3781.012..... | 31844.124 | od | 4.5 | 5403.688 | ev | 3.5 | 10.3 ± 0.5 | −0.66 |
| 3784.472..... | 33565.895 | od | 4.5 | 7149.630 | ev | 5.5 | 0.148 ± 0.022 | −2.50 |
| 3786.836..... | 26399.775 | od | 5.5 | 0.000 | ev | 6.5 | 11.7 ± 0.6 | −0.52 |
| 3787.375..... | 37438.656 | od | 4.5 | 11042.640 | ev | 4.5 | 8.9 ± 0.6 | −0.72 |
| 3791.034..... | 33565.895 | od | 4.5 | 7195.355 | ev | 4.5 | 0.30 ± 0.04 | −2.19 |
| 3791.828..... | 26805.448 | od | 5.5 | 440.434 | ev | 5.5 | 4.63 ± 0.24 | −0.92 |
| 3794.865..... | 33539.273 | od | 3.5 | 7195.355 | ev | 4.5 | 0.21 ± 0.03 | −2.44 |
| 3797.057..... | 26769.141 | od | 6.5 | 440.434 | ev | 5.5 | 3.07 ± 0.15 | −1.03 |
| 3806.054..... | 40547.199 | ev | 8.5 | 14280.723 | od | 7.5 | 6.2 ± 0.7 | −0.61 |
| 3807.999..... | 31385.667 | od | 5.5 | 5132.608 | ev | 4.5 | 0.43 ± 0.05 | −1.95 |
| 3828.569..... | 33307.365 | od | 3.5 | 7195.355 | ev | 4.5 | 0.271 ± 0.029 | −2.32 |
| 3830.482..... | 26098.972 | od | 6.5 | 0.000 | ev | 6.5 | 19.4 ± 1.0 | −0.22 |
| 3832.586..... | 39804.224 | ev | 7.5 | 13719.584 | od | 8.5 | 5.3 ± 0.4 | −0.73 |
| 3841.787..... | 39082.884 | ev | 6.5 | 13060.715 | od | 6.5 | 4.9 ± 0.4 | −0.82 |
| 3851.086..... | 26399.775 | od | 5.5 | 440.434 | ev | 5.5 | 0.364 ± 0.019 | −2.01 |
| 3851.596..... | 33105.534 | od | 5.5 | 7149.630 | ev | 5.5 | 8.6 ± 0.4 | −0.64 |
| 3858.393..... | 33105.534 | od | 5.5 | 7195.355 | ev | 4.5 | 18.5 ± 0.9 | −0.30 |
| 3863.077..... | 33028.394 | od | 4.5 | 7149.630 | ev | 5.5 | 5.3 ± 0.3 | −0.93 |
| 3864.802..... | 36761.150 | od | 4.5 | 10893.936 | ev | 3.5 | 23.3 ± 1.4 | −0.28 |
| 3865.452..... | 33012.493 | od | 6.5 | 7149.630 | ev | 5.5 | 0.20 ± 0.04 | −2.20 |
| 3880.611..... | 30894.447 | od | 3.5 | 5132.608 | ev | 4.5 | 31.3 ± 1.6 | −0.25 |
| 3882.886..... | 32896.371 | od | 4.5 | 7149.630 | ev | 5.5 | 31.6 ± 1.6 | −0.15 |

TABLE 3—*Continued*

| $\lambda_{air}$ (Å) | $E_{upper}$ ($cm^{-1}$) | Parity | $J_{upp}$ | $E_{lower}$ ($cm^{-1}$) | Parity | $J_{low}$ | $A$-value ($10^6$ $s^{-1}$) | log ($gf$) |
|---|---|---|---|---|---|---|---|---|
| 3887.149..... | 36761.150 | od | 4.5 | 11042.640 | ev | 4.5 | 10.1 ± 0.7 | −0.64 |
| 3889.795..... | 32896.371 | od | 4.5 | 7195.355 | ev | 4.5 | 4.99 ± 0.25 | −0.95 |
| 3895.803..... | 32811.006 | od | 5.5 | 7149.630 | ev | 5.5 | 4.46 ± 0.23 | −0.91 |
| 3896.234..... | 26098.972 | od | 6.5 | 440.434 | ev | 5.5 | 23.9 ± 1.2 | −0.12 |
| 3902.758..... | 32811.006 | od | 5.5 | 7195.355 | ev | 4.5 | 8.8 ± 0.4 | −0.62 |
| 3906.312..... | 25592.343 | od | 5.5 | 0.000 | ev | 6.5 | 48.2 ± 2.4 | 0.12 |
| 3918.346..... | 30917.436 | od | 4.5 | 5403.688 | ev | 3.5 | 2.77 ± 0.19 | −1.20 |
| 3921.880..... | 30894.447 | od | 3.5 | 5403.688 | ev | 3.5 | 6.0 ± 0.3 | −0.95 |
| 3939.186..... | 32528.401 | od | 6.5 | 7149.630 | ev | 5.5 | 0.31 ± 0.04 | −1.99 |
| 3943.182..... | 32502.680 | od | 4.5 | 7149.630 | ev | 5.5 | 3.38 ± 0.19 | −1.10 |
| 3950.307..... | 32502.680 | od | 4.5 | 7195.355 | ev | 4.5 | 0.170 ± 0.015 | −2.40 |
| 3969.437..... | 30317.974 | od | 4.5 | 5132.608 | ev | 4.5 | 2.96 ± 0.22 | −1.16 |
| 3974.717..... | 25592.343 | od | 5.5 | 440.434 | ev | 5.5 | 4.93 ± 0.25 | −0.85 |
| 3980.144..... | 32267.246 | od | 4.5 | 7149.630 | ev | 5.5 | 3.13 ± 0.18 | −1.13 |
| 3994.853..... | 30157.742 | od | 5.5 | 5132.608 | ev | 4.5 | 0.41 ± 0.03 | −1.93 |
| 4000.417..... | 30122.939 | od | 5.5 | 5132.608 | ev | 4.5 | 0.228 ± 0.018 | −2.18 |
| 4011.107..... | 32073.360 | od | 5.5 | 7149.630 | ev | 5.5 | 0.193 ± 0.020 | −2.25 |
| 4012.627..... | 30317.974 | od | 4.5 | 5403.688 | ev | 3.5 | 1.26 ± 0.10 | −1.52 |
| 4015.573..... | 30028.618 | od | 4.5 | 5132.608 | ev | 4.5 | 3.63 ± 0.18 | −1.06 |
| 4017.355..... | 35927.604 | od | 3.5 | 11042.640 | ev | 4.5 | 1.53 ± 0.12 | −1.53 |
| 4018.479..... | 32073.360 | od | 5.5 | 7195.355 | ev | 4.5 | 0.60 ± 0.05 | −1.76 |
| 4043.162..... | 29858.739 | od | 5.5 | 5132.608 | ev | 4.5 | 0.050 ± 0.005 | −2.83 |
| 4048.342..... | 31844.124 | od | 4.5 | 7149.630 | ev | 5.5 | 5.6 ± 0.3 | −0.86 |
| 4055.407..... | 31801.102 | od | 5.5 | 7149.630 | ev | 5.5 | 1.08 ± 0.09 | −1.50 |
| 4055.464..... | 29783.733 | od | 4.5 | 5132.608 | ev | 4.5 | 10.3 ± 0.5 | −0.60 |
| 4055.852..... | 31844.124 | od | 4.5 | 7195.355 | ev | 4.5 | 1.69 ± 0.11 | −1.38 |
| 4059.779..... | 30028.618 | od | 4.5 | 5403.688 | ev | 3.5 | 6.2 ± 0.3 | −0.81 |
| 4062.944..... | 31801.102 | od | 5.5 | 7195.355 | ev | 4.5 | 0.89 ± 0.08 | −1.58 |
| 4100.558..... | 29783.733 | od | 4.5 | 5403.688 | ev | 3.5 | 4.81 ± 0.24 | −0.92 |
| 4103.979..... | 29492.329 | od | 5.5 | 5132.608 | ev | 4.5 | 0.49 ± 0.03 | −1.83 |
| 4112.615..... | 41244.400 | ev | 8.5 | 16935.832 | od | 9.5 | 9.2 ± 1.1 | −0.38 |
| 4132.721..... | 31385.667 | od | 5.5 | 7195.355 | ev | 4.5 | 0.154 ± 0.020 | −2.32 |
| 4135.654..... | 36761.150 | od | 4.5 | 12587.998 | ev | 3.5 | 0.89 ± 0.11 | −1.64 |
| 4135.707..... | 35215.487 | od | 5.5 | 11042.640 | ev | 4.5 | 0.31 ± 0.04 | −2.03 |
| 4142.914..... | 29263.402 | od | 3.5 | 5132.608 | ev | 4.5 | 9.2 ± 0.5 | −0.72 |
| 4186.704..... | 29011.015 | od | 4.5 | 5132.608 | ev | 4.5 | 0.41 ± 0.03 | −1.97 |
| 4189.984..... | 29263.402 | od | 3.5 | 5403.688 | ev | 3.5 | 4.59 ± 0.23 | −1.01 |
| 4201.241..... | 41174.705 | ev | 7.5 | 17378.917 | od | 6.5 | 1.52 ± 0.27 | −1.19 |
| 4206.187..... | 30917.436 | od | 4.5 | 7149.630 | ev | 5.5 | 0.140 ± 0.016 | −2.43 |
| 4214.295..... | 30917.436 | od | 4.5 | 7195.355 | ev | 4.5 | 0.107 ± 0.012 | −2.54 |
| 4234.056..... | 40547.199 | ev | 8.5 | 16935.832 | od | 9.5 | 0.51 ± 0.07 | −1.61 |
| 4234.781..... | 29011.015 | od | 4.5 | 5403.688 | ev | 3.5 | 1.14 ± 0.08 | −1.51 |
| 4253.541..... | 34397.143 | od | 4.5 | 10893.936 | ev | 3.5 | 0.28 ± 0.03 | −2.12 |
| 4280.625..... | 34397.143 | od | 4.5 | 11042.640 | ev | 4.5 | 0.219 ± 0.024 | −2.22 |
| 4285.578..... | 35927.604 | od | 3.5 | 12600.093 | ev | 2.5 | 0.75 ± 0.08 | −1.78 |
| 4290.187..... | 34196.388 | od | 4.5 | 10893.936 | ev | 3.5 | 0.157 ± 0.027 | −2.36 |
| 4301.596..... | 23240.649 | od | 5.5 | 0.000 | ev | 6.5 | 0.85 ± 0.04 | −1.55 |
| 4303.208..... | 35819.939 | od | 3.5 | 12587.998 | ev | 3.5 | 0.37 ± 0.04 | −2.08 |
| 4303.794..... | 28361.386 | od | 5.5 | 5132.608 | ev | 4.5 | 0.185 ± 0.019 | −2.21 |
| 4305.450..... | 35819.939 | od | 3.5 | 12600.093 | ev | 2.5 | 0.46 ± 0.05 | −1.99 |
| 4315.021..... | 30317.974 | od | 4.5 | 7149.630 | ev | 5.5 | 0.123 ± 0.015 | −2.46 |
| 4316.391..... | 39804.224 | ev | 7.5 | 16643.237 | od | 6.5 | 1.23 ± 0.14 | −1.26 |
| 4317.741..... | 34196.388 | od | 4.5 | 11042.640 | ev | 4.5 | 0.071 ± 0.011 | −2.70 |
| 4323.554..... | 30317.974 | od | 4.5 | 7195.355 | ev | 4.5 | 0.027 ± 0.006 | −3.12 |
| 4345.072..... | 30157.742 | od | 5.5 | 7149.630 | ev | 5.5 | 0.150 ± 0.015 | −2.29 |
| 4353.724..... | 30157.742 | od | 5.5 | 7195.355 | ev | 4.5 | 0.015 ± 0.002 | −3.29 |
| 4369.595..... | 30028.618 | od | 4.5 | 7149.630 | ev | 5.5 | 0.463 ± 0.027 | −1.88 |
| 4378.345..... | 30028.618 | od | 4.5 | 7195.355 | ev | 4.5 | 0.58 ± 0.03 | −1.78 |
| 4384.692..... | 23240.649 | od | 5.5 | 440.434 | ev | 5.5 | 0.88 ± 0.04 | −1.52 |
| 4388.380..... | 41244.400 | ev | 8.5 | 18463.347 | od | 7.5 | 5.4 ± 0.8 | −0.55 |
| 4401.847..... | 41174.705 | ev | 7.5 | 18463.347 | od | 7.5 | 1.66 ± 0.25 | −1.11 |
| 4402.283..... | 29858.739 | od | 5.5 | 7149.630 | ev | 5.5 | 0.016 ± 0.003 | −3.26 |
| 4403.173..... | 40547.199 | ev | 8.5 | 17842.682 | od | 8.5 | 4.7 ± 0.6 | −0.61 |
| 4414.680..... | 33539.273 | od | 3.5 | 10893.936 | ev | 3.5 | 0.151 ± 0.018 | −2.45 |
| 4416.871..... | 29783.733 | od | 4.5 | 7149.630 | ev | 5.5 | 0.053 ± 0.007 | −2.81 |

TABLE 3—*Continued*

| $\lambda_{air}$ (Å) | $E_{upper}$ ($cm^{-1}$) | Parity | $J_{upp}$ | $E_{lower}$ ($cm^{-1}$) | Parity | $J_{low}$ | $A$-value ($10^6$ $s^{-1}$) | log ($gf$) |
|---|---|---|---|---|---|---|---|---|
| 4420.232 | 33659.536 | od | 5.5 | 11042.640 | ev | 4.5 | 0.025 ± 0.004 | −3.06 |
| 4425.813 | 29783.733 | od | 4.5 | 7195.355 | ev | 4.5 | 0.092 ± 0.008 | −2.57 |
| 4432.663 | 39082.884 | ev | 6.5 | 16529.413 | od | 5.5 | 1.35 ± 0.15 | −1.25 |
| 4438.609 | 33565.895 | od | 4.5 | 11042.640 | ev | 4.5 | 0.068 ± 0.011 | −2.70 |
| 4441.213 | 27642.658 | od | 5.5 | 5132.608 | ev | 4.5 | 0.183 ± 0.017 | −2.19 |
| 4457.997 | 39804.224 | ev | 7.5 | 17378.917 | od | 6.5 | 0.68 ± 0.07 | −1.49 |
| 4460.359 | 33307.365 | od | 3.5 | 10893.936 | ev | 3.5 | 0.126 ± 0.013 | −2.52 |
| 4474.479 | 29492.329 | od | 5.5 | 7149.630 | ev | 5.5 | 0.232 ± 0.023 | −2.08 |
| 4480.169 | 34902.323 | od | 3.5 | 12587.998 | ev | 3.5 | 0.71 ± 0.07 | −1.77 |
| 4482.599 | 34902.323 | od | 3.5 | 12600.093 | ev | 2.5 | 0.35 ± 0.04 | −2.07 |
| 4483.655 | 29492.329 | od | 5.5 | 7195.355 | ev | 4.5 | 0.291 ± 0.027 | −1.98 |
| 4490.150 | 33307.365 | od | 3.5 | 11042.640 | ev | 4.5 | 0.70 ± 0.07 | −1.77 |
| 4526.926 | 40547.199 | ev | 8.5 | 18463.347 | od | 7.5 | 3.8 ± 0.5 | −0.68 |
| 4540.229 | 39082.884 | ev | 6.5 | 17063.735 | od | 5.5 | 1.37 ± 0.16 | −1.23 |
| 4550.391 | 29119.606 | od | 6.5 | 7149.630 | ev | 5.5 | 0.072 ± 0.007 | −2.51 |
| 4552.138 | 39804.224 | ev | 7.5 | 17842.682 | od | 8.5 | 10.7 ± 0.8 | −0.28 |
| 4572.994 | 29011.015 | od | 4.5 | 7149.630 | ev | 5.5 | 0.236 ± 0.023 | −2.13 |
| 4574.596 | 32896.371 | od | 4.5 | 11042.640 | ev | 4.5 | 0.181 ± 0.027 | −2.24 |
| 4583.948 | 34397.143 | od | 4.5 | 12587.998 | ev | 3.5 | 0.137 ± 0.016 | −2.37 |
| 4615.866 | 40121.685 | ev | 6.5 | 18463.347 | od | 7.5 | 1.12 ± 0.16 | −1.30 |
| 4700.768 | 26399.775 | od | 5.5 | 5132.608 | ev | 4.5 | 0.037 ± 0.004 | −2.83 |
| 4723.230 | 28361.386 | od | 5.5 | 7195.355 | ev | 4.5 | 0.152 ± 0.016 | −2.21 |
| 4774.104 | 40547.199 | ev | 8.5 | 19606.715 | od | 8.5 | 0.40 ± 0.11 | −1.61 |
| 4815.967 | 31801.102 | od | 5.5 | 11042.640 | ev | 4.5 | 0.016 ± 0.003 | −3.17 |
| 4839.625 | 41174.705 | ev | 7.5 | 20517.717 | od | 7.5 | 0.88 ± 0.17 | −1.31 |
| 4848.415 | 39082.884 | ev | 6.5 | 18463.347 | od | 7.5 | 2.29 ± 0.27 | −0.95 |
| 4886.284 | 25592.343 | od | 5.5 | 5132.608 | ev | 4.5 | 0.41 ± 0.04 | −1.75 |
| 4889.255 | 27642.658 | od | 5.5 | 7195.355 | ev | 4.5 | 0.049 ± 0.006 | −2.68 |
| 4909.274 | 27513.555 | od | 6.5 | 7149.630 | ev | 5.5 | 0.093 ± 0.013 | −2.33 |
| 4922.703 | 32896.371 | od | 4.5 | 12587.998 | ev | 3.5 | 0.142 ± 0.016 | −2.29 |
| 4949.724 | 39804.224 | ev | 7.5 | 19606.715 | od | 8.5 | 1.25 ± 0.17 | −1.13 |
| 4956.316 | 41174.705 | ev | 7.5 | 21004.060 | od | 6.5 | 1.22 ± 0.22 | −1.14 |
| 4966.623 | 40121.685 | ev | 6.5 | 19992.895 | od | 5.5 | 5.6 ± 0.8 | −0.54 |
| 4992.739 | 30917.436 | od | 4.5 | 10893.936 | ev | 3.5 | 0.125 ± 0.018 | −2.33 |
| 5097.994 | 26805.448 | od | 5.5 | 7195.355 | ev | 4.5 | 0.062 ± 0.010 | −2.54 |
| 5099.587 | 40121.685 | ev | 6.5 | 20517.717 | od | 7.5 | 0.71 ± 0.12 | −1.41 |
| 5183.528 | 39804.224 | ev | 7.5 | 20517.717 | od | 7.5 | 1.10 ± 0.12 | −1.15 |
| 5193.320 | 26399.775 | od | 5.5 | 7149.630 | ev | 5.5 | 0.035 ± 0.004 | −2.77 |
| 5224.658 | 30028.618 | od | 4.5 | 10893.936 | ev | 3.5 | 0.035 ± 0.010 | −2.85 |
| 5292.391 | 29783.733 | od | 4.5 | 10893.936 | ev | 3.5 | 0.123 ± 0.014 | −2.29 |
| 5317.623 | 39804.224 | ev | 7.5 | 21004.060 | od | 6.5 | 0.76 ± 0.10 | −1.29 |
| 5414.189 | 40121.685 | ev | 6.5 | 21656.831 | od | 5.5 | 0.98 ± 0.18 | −1.22 |
| 5434.162 | 25592.343 | od | 5.5 | 7195.355 | ev | 4.5 | 0.043 ± 0.008 | −2.64 |
| 5462.434 | 40121.685 | ev | 6.5 | 21819.914 | od | 5.5 | 4.4 ± 0.8 | −0.56 |
| 5518.121 | 29011.015 | od | 4.5 | 10893.936 | ev | 3.5 | 0.157 ± 0.029 | −2.14 |
| 5529.797 | 39082.884 | ev | 6.5 | 21004.060 | od | 6.5 | 0.51 ± 0.08 | −1.49 |
| 5710.870 | 41174.705 | ev | 7.5 | 23669.096 | od | 6.5 | 3.1 ± 0.6 | −0.61 |
| 5788.607 | 41244.400 | ev | 8.5 | 23973.877 | od | 7.5 | 1.08 ± 0.21 | −1.01 |
| 5791.140 | 39082.884 | ev | 6.5 | 21819.914 | od | 5.5 | 1.8 ± 0.3 | −0.90 |
| 5812.062 | 41174.705 | ev | 7.5 | 23973.877 | od | 7.5 | 1.3 ± 0.3 | −0.99 |
| 5844.055 | 33659.536 | od | 5.5 | 16552.871 | ev | 4.5 | 0.19 ± 0.04 | −1.93 |
| 6045.633 | 41244.400 | ev | 8.5 | 24708.113 | od | 9.5 | 1.8 ± 0.4 | −0.76 |
| 6061.249 | 40547.199 | ev | 8.5 | 24053.517 | od | 8.5 | 1.30 ± 0.27 | −0.89 |
| 6267.934 | 32502.680 | od | 4.5 | 16552.871 | ev | 4.5 | 0.43 ± 0.06 | −1.59 |
| 6311.750 | 40547.199 | ev | 8.5 | 24708.113 | od | 9.5 | 0.13 ± 0.03 | −1.84 |
| 6347.166 | 39804.224 | ev | 7.5 | 24053.517 | od | 8.5 | 2.7 ± 0.4 | −0.58 |
| 6509.833 | 26399.775 | od | 5.5 | 11042.640 | ev | 4.5 | 0.008 ± 0.001 | −3.21 |
| 6556.327 | 31801.102 | od | 5.5 | 16552.871 | ev | 4.5 | 0.27 ± 0.06 | −1.68 |
| 6616.741 | 39082.884 | ev | 6.5 | 23973.877 | od | 7.5 | 2.1 ± 0.4 | −0.71 |
| 6740.117 | 33721.545 | od | 5.5 | 18889.101 | ev | 5.5 | 0.085 ± 0.020 | −2.16 |
| 6761.677 | 33674.250 | od | 6.5 | 18889.101 | ev | 5.5 | 0.37 ± 0.07 | −1.45 |
| 6768.413 | 33659.536 | od | 5.5 | 18889.101 | ev | 5.5 | 0.27 ± 0.04 | −1.66 |
| 6944.942 | 33012.493 | od | 6.5 | 18617.495 | ev | 7.5 | 0.16 ± 0.03 | −1.79 |
| 7329.735 | 32528.401 | od | 6.5 | 18889.101 | ev | 5.5 | 0.58 ± 0.11 | −1.18 |
| 7348.284 | 30157.742 | od | 5.5 | 16552.871 | ev | 4.5 | 0.082 ± 0.015 | −2.10 |

TABLE 3—*Continued*

| $\lambda_{air}$ (Å) | $E_{upper}$ ($cm^{-1}$) | Parity | $J_{upp}$ | $E_{lower}$ ($cm^{-1}$) | Parity | $J_{low}$ | $A$-value ($10^6$ $s^{-1}$) | log ($gf$) |
|---|---|---|---|---|---|---|---|---|
| 7367.130..... | 30122.939 | od | 5.5 | 16552.871 | ev | 4.5 | 0.071 ± 0.013 | −2.16 |
| 7513.412..... | 29858.739 | od | 5.5 | 16552.871 | ev | 4.5 | 0.038 ± 0.008 | −2.41 |
| 7556.006..... | 29783.733 | od | 4.5 | 16552.871 | ev | 4.5 | 0.058 ± 0.010 | −2.30 |
| 7694.178..... | 32896.371 | od | 4.5 | 19903.107 | ev | 3.5 | 0.21 ± 0.03 | −1.73 |
| 7726.173..... | 29492.329 | od | 5.5 | 16552.871 | ev | 4.5 | 0.118 ± 0.021 | −1.90 |
| 7742.602..... | 31801.102 | od | 5.5 | 18889.101 | ev | 5.5 | 0.043 ± 0.011 | −2.33 |
| 7934.594..... | 32502.680 | od | 4.5 | 19903.107 | ev | 3.5 | 0.080 ± 0.015 | −2.12 |
| 7999.998..... | 31385.667 | od | 5.5 | 18889.101 | ev | 5.5 | 0.119 ± 0.025 | −1.86 |
| 8085.683..... | 32267.246 | od | 4.5 | 19903.107 | ev | 3.5 | 0.076 ± 0.014 | −2.13 |
| 8328.540..... | 30621.102 | od | 6.5 | 18617.495 | ev | 7.5 | 0.73 ± 0.16 | −0.97 |
| 8466.139..... | 28361.386 | od | 5.5 | 16552.871 | ev | 4.5 | 0.18 ± 0.03 | −1.63 |
| 8521.354..... | 30621.102 | od | 6.5 | 18889.101 | ev | 5.5 | 0.57 ± 0.12 | −1.06 |
| 8708.910..... | 33012.493 | od | 6.5 | 21533.153 | ev | 7.5 | 0.108 ± 0.025 | −1.77 |
| 8871.749..... | 30157.742 | od | 5.5 | 18889.101 | ev | 5.5 | 0.037 ± 0.008 | −2.28 |
| 9014.831..... | 27642.658 | od | 5.5 | 16552.871 | ev | 4.5 | 0.43 ± 0.08 | −1.20 |
| 9069.148..... | 29640.863 | od | 7.5 | 18617.495 | ev | 7.5 | 0.14 ± 0.03 | −1.56 |
| 9072.496..... | 34902.323 | od | 3.5 | 23883.022 | ev | 2.5 | 0.072 ± 0.018 | −2.15 |
| 9076.591..... | 30917.436 | od | 4.5 | 19903.107 | ev | 3.5 | 0.17 ± 0.04 | −1.68 |
| 9092.342..... | 32528.401 | od | 6.5 | 21533.153 | ev | 7.5 | 0.25 ± 0.06 | −1.36 |
| 9176.314..... | 29783.733 | od | 4.5 | 18889.101 | ev | 5.5 | 0.031 ± 0.006 | −2.40 |
| 9196.145..... | 33012.493 | od | 6.5 | 22141.355 | ev | 6.5 | 0.056 ± 0.014 | −2.00 |
| 9209.568..... | 29472.789 | od | 7.5 | 18617.495 | ev | 7.5 | 0.19 ± 0.04 | −1.42 |
| 9309.036..... | 29628.405 | od | 6.5 | 18889.101 | ev | 5.5 | 0.17 ± 0.03 | −1.51 |
| 9380.387..... | 31385.667 | od | 5.5 | 20728.050 | ev | 6.5 | 0.25 ± 0.05 | −1.40 |
| 9428.504..... | 29492.329 | od | 5.5 | 18889.101 | ev | 5.5 | 0.069 ± 0.015 | −1.96 |
| 9519.284..... | 29119.606 | od | 6.5 | 18617.495 | ev | 7.5 | 0.080 ± 0.016 | −1.82 |
| 9530.677..... | 37438.656 | od | 4.5 | 26949.099 | ev | 3.5 | 0.26 ± 0.06 | −1.46 |
| 9599.026..... | 30317.974 | od | 4.5 | 19903.107 | ev | 3.5 | 0.64 ± 0.15 | −1.05 |
| 9670.370..... | 29640.863 | od | 7.5 | 19302.832 | ev | 8.5 | 5.3 ± 1.1 | 0.08 |
| 9750.971..... | 26805.448 | od | 5.5 | 16552.871 | ev | 4.5 | 0.58 ± 0.10 | −1.00 |
| 9830.188..... | 29472.789 | od | 7.5 | 19302.832 | ev | 8.5 | 0.66 ± 0.13 | −0.82 |
| 9895.092..... | 31801.102 | od | 5.5 | 21697.852 | ev | 5.5 | 0.037 ± 0.009 | −2.18 |
| 10091.059..... | 31801.102 | od | 5.5 | 21894.055 | ev | 4.5 | 0.021 ± 0.005 | −2.41 |
| 10105.334..... | 30621.102 | od | 6.5 | 20728.050 | ev | 6.5 | 0.062 ± 0.015 | −1.87 |
| 10152.693..... | 26399.775 | od | 5.5 | 16552.871 | ev | 4.5 | 0.17 ± 0.04 | −1.50 |
| 10319.417..... | 31385.667 | od | 5.5 | 21697.852 | ev | 5.5 | 0.92 ± 0.20 | −0.75 |
| 10349.402..... | 31801.102 | od | 5.5 | 22141.355 | ev | 6.5 | 0.050 ± 0.012 | −2.01 |
| 10532.732..... | 31385.667 | od | 5.5 | 21894.055 | ev | 4.5 | 0.42 ± 0.10 | −1.07 |
| 10554.223..... | 28361.386 | od | 5.5 | 18889.101 | ev | 5.5 | 0.062 ± 0.013 | −1.91 |
| 10601.896..... | 30157.742 | od | 5.5 | 20728.050 | ev | 6.5 | 0.043 ± 0.010 | −2.06 |
| 10641.170..... | 30122.939 | od | 5.5 | 20728.050 | ev | 6.5 | 0.14 ± 0.03 | −1.54 |
| 10843.506..... | 30917.436 | od | 4.5 | 21697.852 | ev | 5.5 | 0.077 ± 0.018 | −1.87 |
| 10976.463..... | 29011.015 | od | 4.5 | 19903.107 | ev | 3.5 | 0.84 ± 0.18 | −0.82 |
| 11000.570..... | 30621.102 | od | 6.5 | 21533.153 | ev | 7.5 | 0.96 ± 0.22 | −0.61 |
| 11059.564..... | 25592.343 | od | 5.5 | 16552.871 | ev | 4.5 | 1.05 ± 0.19 | −0.64 |
| 11216.731..... | 29640.863 | od | 7.5 | 20728.050 | ev | 6.5 | 0.14 ± 0.04 | −1.37 |
| 11232.431..... | 29628.405 | od | 6.5 | 20728.050 | ev | 6.5 | 0.045 ± 0.012 | −1.92 |
| 11237.854..... | 27513.555 | od | 6.5 | 18617.495 | ev | 7.5 | 1.48 ± 0.30 | −0.41 |
| 11420.801..... | 27642.658 | od | 5.5 | 18889.101 | ev | 5.5 | 0.14 ± 0.03 | −1.49 |
| 11432.317..... | 29472.789 | od | 7.5 | 20728.050 | ev | 6.5 | 0.056 ± 0.014 | −1.76 |
| 11591.764..... | 27513.555 | od | 6.5 | 18889.101 | ev | 5.5 | 0.034 ± 0.009 | −2.01 |
| 11597.589..... | 30317.974 | od | 4.5 | 21697.852 | ev | 5.5 | 0.108 ± 0.028 | −1.66 |
| 11789.578..... | 30621.102 | od | 6.5 | 22141.355 | ev | 6.5 | 0.52 ± 0.13 | −0.82 |
| 11817.250..... | 30157.742 | od | 5.5 | 21697.852 | ev | 5.5 | 0.13 ± 0.03 | −1.48 |
| 11866.066..... | 30122.939 | od | 5.5 | 21697.852 | ev | 5.5 | 0.106 ± 0.026 | −1.57 |
| 11867.711..... | 30317.974 | od | 4.5 | 21894.055 | ev | 4.5 | 0.27 ± 0.07 | −1.25 |
| 12097.825..... | 30157.742 | od | 5.5 | 21894.055 | ev | 4.5 | 0.082 ± 0.020 | −1.67 |
| 12330.565..... | 29640.863 | od | 7.5 | 21533.153 | ev | 7.5 | 0.72 ± 0.19 | −0.58 |
| 12349.541..... | 29628.405 | od | 6.5 | 21533.153 | ev | 7.5 | 0.13 ± 0.03 | −1.39 |
| 12471.036..... | 30157.742 | od | 5.5 | 22141.355 | ev | 6.5 | 0.057 ± 0.015 | −1.79 |
| 12525.415..... | 30122.939 | od | 5.5 | 22141.355 | ev | 6.5 | 0.053 ± 0.014 | −1.82 |
| 12591.591..... | 29472.789 | od | 7.5 | 21533.153 | ev | 7.5 | 0.086 ± 0.022 | −1.48 |
| 12591.978..... | 32502.680 | od | 4.5 | 24563.288 | ev | 4.5 | 0.071 ± 0.018 | −1.77 |
| 12628.634..... | 26805.448 | od | 5.5 | 18889.101 | ev | 5.5 | 0.134 ± 0.030 | −1.41 |
| 12727.096..... | 32896.371 | od | 4.5 | 25041.268 | ev | 3.5 | 0.18 ± 0.04 | −1.37 |

TABLE 3—*Continued*

| $\lambda_{air}$ (Å) | $E_{upper}$ ($cm^{-1}$) | Parity | $J_{upp}$ | $E_{lower}$ ($cm^{-1}$) | Parity | $J_{low}$ | *A*-value ($10^6$ $s^{-1}$) | log (*gf*) |
|---|---|---|---|---|---|---|---|---|
| 12826.089..... | 29492.329 | od | 5.5 | 21697.852 | ev | 5.5 | 0.071 ± 0.017 | −1.68 |
| 12886.983..... | 32502.680 | od | 4.5 | 24745.034 | ev | 5.5 | 0.086 ± 0.022 | −1.67 |
| 12976.791..... | 32267.246 | od | 4.5 | 24563.288 | ev | 4.5 | 0.065 ± 0.018 | −1.79 |
| 13096.850..... | 28361.386 | od | 5.5 | 20728.050 | ev | 6.5 | 0.007 ± 0.002 | −2.65 |
| 13157.285..... | 29492.329 | od | 5.5 | 21894.055 | ev | 4.5 | 0.039 ± 0.010 | −1.91 |
| 13290.327..... | 32267.246 | od | 4.5 | 24745.034 | ev | 5.5 | 0.073 ± 0.019 | −1.72 |
| 13310.744..... | 26399.775 | od | 5.5 | 18889.101 | ev | 5.5 | 0.055 ± 0.013 | −1.75 |
| 13330.563..... | 29640.863 | od | 7.5 | 22141.355 | ev | 6.5 | 0.064 ± 0.017 | −1.56 |
| 13352.744..... | 29628.405 | od | 6.5 | 22141.355 | ev | 6.5 | 0.050 ± 0.013 | −1.73 |
| 13670.236..... | 29011.015 | od | 4.5 | 21697.852 | ev | 5.5 | 0.20 ± 0.05 | −1.25 |
| 14047.103..... | 29011.015 | od | 4.5 | 21894.055 | ev | 4.5 | 0.30 ± 0.08 | −1.05 |
| 14733.270..... | 27513.555 | od | 6.5 | 20728.050 | ev | 6.5 | 0.16 ± 0.04 | −1.15 |
| 15002.952..... | 28361.386 | od | 5.5 | 21697.852 | ev | 5.5 | 0.054 ± 0.013 | −1.66 |
| 15458.105..... | 28361.386 | od | 5.5 | 21894.055 | ev | 4.5 | 0.023 ± 0.005 | −2.01 |
| 16072.699..... | 28361.386 | od | 5.5 | 22141.355 | ev | 6.5 | 0.060 ± 0.015 | −1.55 |
| 16449.917..... | 26805.448 | od | 5.5 | 20728.050 | ev | 6.5 | 0.043 ± 0.010 | −1.68 |
| 16716.718..... | 27513.555 | od | 6.5 | 21533.153 | ev | 7.5 | 0.014 ± 0.004 | −2.08 |
| 17173.441..... | 29783.733 | od | 4.5 | 23962.378 | ev | 3.5 | 0.019 ± 0.005 | −2.08 |
| 17190.131..... | 27513.555 | od | 6.5 | 21697.852 | ev | 5.5 | 0.035 ± 0.009 | −1.67 |
| 17372.398..... | 30317.974 | od | 4.5 | 24563.288 | ev | 4.5 | 0.012 ± 0.003 | −2.28 |
| 17626.507..... | 26399.775 | od | 5.5 | 20728.050 | ev | 6.5 | 0.012 ± 0.003 | −2.18 |
| 17938.951..... | 30317.974 | od | 4.5 | 24745.034 | ev | 5.5 | 0.019 ± 0.006 | −2.05 |
| 18172.549..... | 27642.658 | od | 5.5 | 22141.355 | ev | 6.5 | 0.013 ± 0.003 | −2.10 |
| 18609.267..... | 27513.555 | od | 6.5 | 22141.355 | ev | 6.5 | 0.047 ± 0.013 | −1.47 |
| 18664.940..... | 32896.371 | od | 4.5 | 27540.195 | ev | 5.5 | 0.076 ± 0.019 | −1.40 |
| 18907.775..... | 32896.371 | od | 4.5 | 27608.985 | ev | 4.5 | 0.054 ± 0.014 | −1.54 |
| 19150.227..... | 29783.733 | od | 4.5 | 24563.288 | ev | 4.5 | 0.044 ± 0.012 | −1.62 |
| 19801.920..... | 29011.015 | od | 4.5 | 23962.378 | ev | 3.5 | 0.034 ± 0.010 | −1.70 |
| 19840.977..... | 29783.733 | od | 4.5 | 24745.034 | ev | 5.5 | 0.064 ± 0.015 | −1.42 |

NOTES.—Table 3 is also available in machine-readable form in the electronic edition of the *Astrophysical Journal Supplement.*

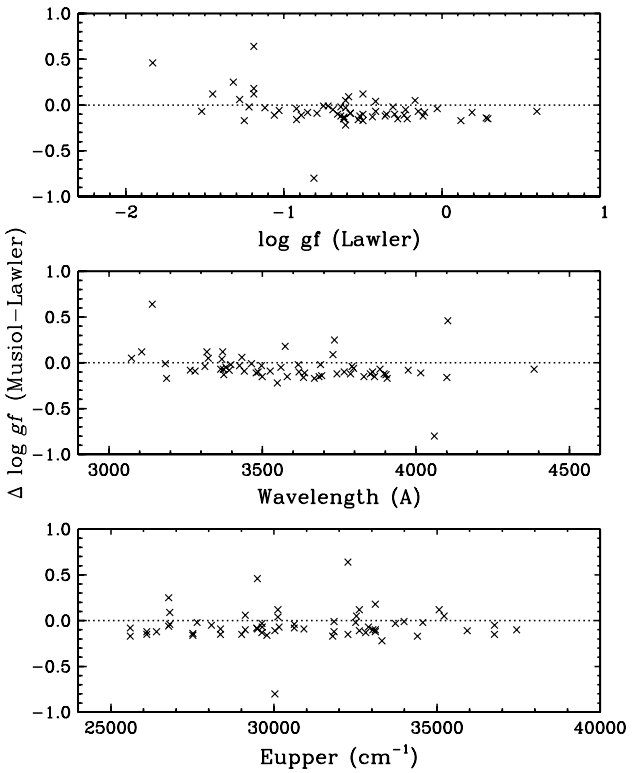


FIG. 4.—Comparison of experimental transition probabilities from Musiol & Labuz (1983) to our transition probabilities as function of our transition probability or log (*gf*), wavelength, and upper level energy.

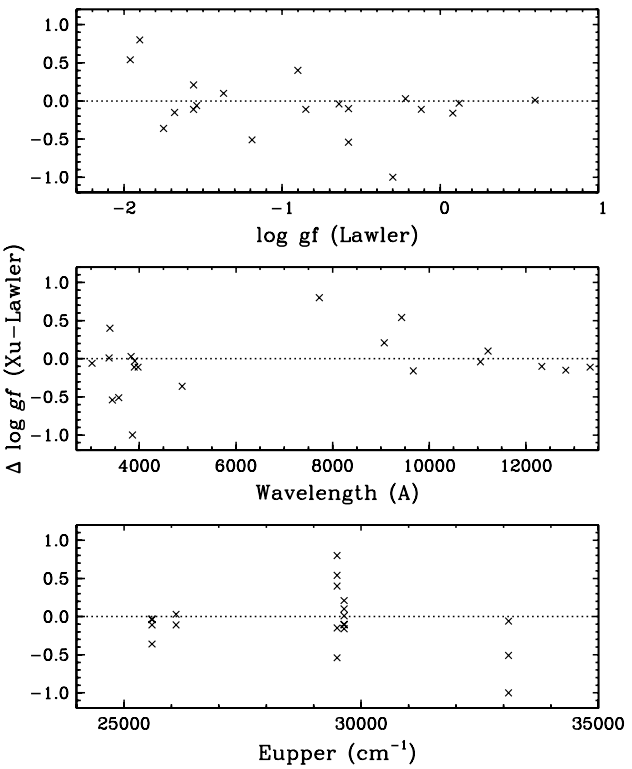


FIG. 5.—Comparison of theoretical transition probabilities from Xu et al. (2003) to our transition probabilities as function of our transition probability or log (*gf*), wavelength, and upper level energy.

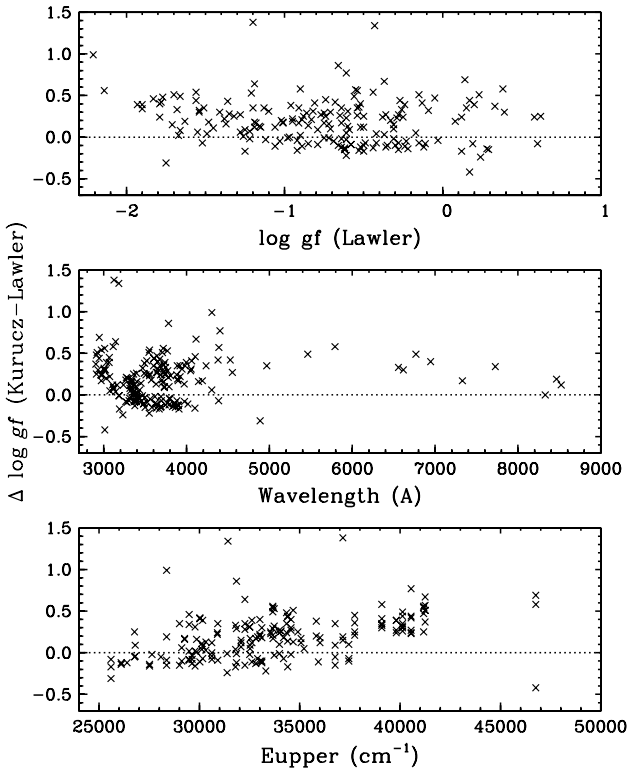


FIG. 6.—Comparison of theoretical transition probabilities from the Kurucz linelist (see footnote 10) to our transition probabilities as function of our transition probability or log ($gf$), wavelength, and upper level energy.

factors. For a line on the linear part of the curve of growth, the relationship between equivalent width (EW), reduced width (RW), transition probability, excitation energy $\chi$ (measured in eV), and inverse temperature $\theta \equiv 5040/T$ is

$$\log(\mathrm{RW}) = \log(\mathrm{EW}/\lambda) = \text{constant} + \log(gf) - \theta\chi.$$

The relative strengths of lines of different species also depend on relative elemental abundances and Saha ionization equilibrium factors. However, the relatively low first ionization potential of Er (6.108 eV; Grigoriev & Melikhov 1997) ensures that it almost entirely exists as Er II in the photospheres of the Sun and stars considered here. Therefore Er II, like those of all rare-earth single ions, needs essentially no Saha corrections for the existence of other ionization states. Thus, for all elements with similarly low ionization potentials their weak-ionized-line strength factors are

$$\mathrm{STR} \equiv \log(\varepsilon gf) - \theta\chi,$$

where $\varepsilon$ is the elemental abundance.

In Figure 7 we plot these relative strength factors as a function of wavelength for Gd II lines (Den Hartog et al. 2006) and Er II lines (this paper). To compute the strength factors we have adopted solar abundances of $\log\varepsilon(\mathrm{Gd}) = +1.11$ (Den Hartog et al.) and $\log\varepsilon(\mathrm{Er}) = +0.95$ (close to the recommended photospheric abundance of Grevesse & Sauval [2002] and Lodders [2003]), which will be the new value derived in this paper. This plot is very similar to ones that we have shown in several of our previous papers. As in those studies, we have used horizontal lines to indicate approximate strength factors for "strong" and "barely detectable" lines as follows.

The minimum detectable strength limit for Sm II lines was estimated by Lawler et al. (2006) by first searching the Delbouille et al. (1973) solar photospheric spectrum for the weakest lines that could be reliably employed in an abundance analysis. That exercise suggested an EW limit of about 1.5 mÅ near $\lambda \sim 4500$ Å, or $\log(\mathrm{RW}) \approx -6.5$. Lines of Sm II near this limit have $\mathrm{STR} = \log(\varepsilon gf) - \theta\chi \approx -0.6$. That EW and thus STR limit should apply also to Gd II and Er II lines, and so it has been indicated in both panels of Figure 7 with horizontal dotted lines.

Minimum strength factors for relatively strong lines were estimated by Lawler et al. (2006) by beginning with the detection-limit

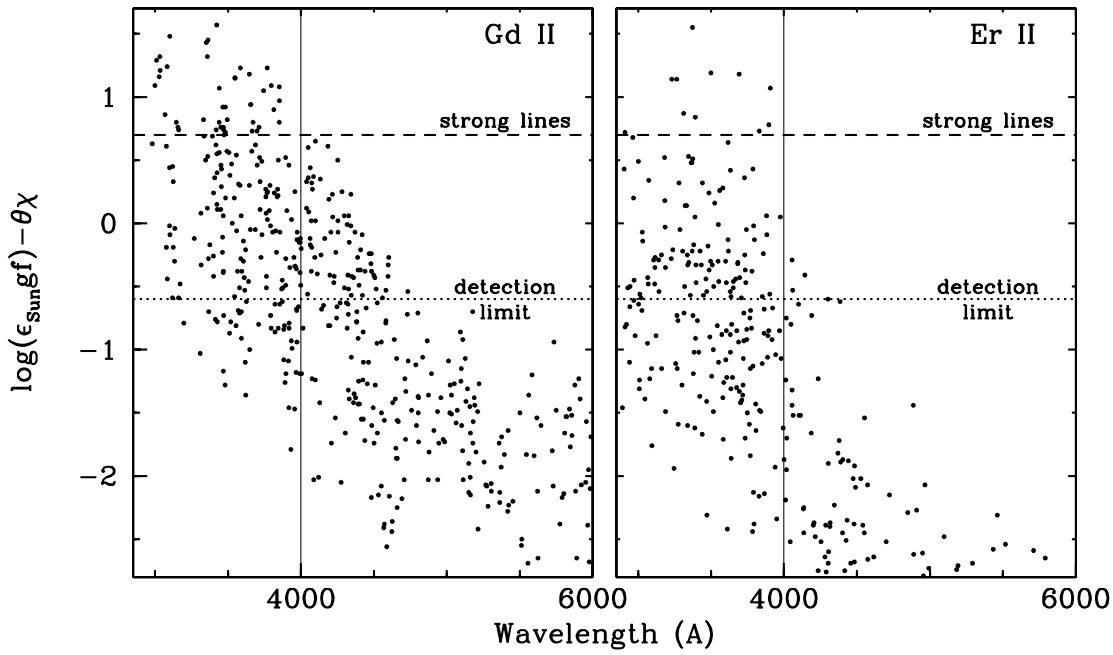


FIG. 7.—Relative transition strength factors, $\mathrm{STR} \equiv \log(\varepsilon gf) - \theta\chi$, for lines of Gd II (Den Hartog et al. 2006) and Er II (this study). For display purposes the long-wavelength limit has been set to 6000 Å, which cuts out only some extremely weak lines of Gd II and Er II that can be detected neither in the Sun nor nearly all other stars. The short-wavelength limit of 2900 Å covers all lines at that end of the spectrum in these two studies. Definitions of "detection limit" and "strong lines" of these species are given in the text.

TABLE 4

ERBIUM ABUNDANCES FROM INDIVIDUAL LINES IN THE SUN AND THE *r*-PROCESS RICH METAL-POOR GIANT STARS

| λ (Å) | E. P. (eV) | log (*gf*) | log ε Sun | log ε CS 22892 | log ε BD +17 3248 | log ε HD 221170 | log ε HD 115444 | log ε CS 31082 | log ε CS 29497 |
|---|---|---|---|---|---|---|---|---|---|
| 3230.58 | 0.055 | 0.24 | 0.98 | −0.49 | −0.36 | ... | −1.26 | −0.32 | 0.59 |
| 3312.42 | 0.055 | −0.03 | ... | −0.47 | −0.23 | ... | −1.21 | −0.27 | 0.64 |
| 3332.70 | 0.886 | 0.07 | 0.90 | −0.48 | ... | ... | ... | −0.29 | ... |
| 3346.02 | 0.055 | −0.37 | ... | −0.42 | −0.24 | −0.33 | −1.33 | ... | ... |
| 3364.07 | 0.055 | −0.42 | 1.01 | −0.52 | ... | ... | ... | −0.34 | ... |
| 3499.11 | 0.055 | 0.29 | ... | −0.52 | −0.29 | −0.48 | −1.28 | −0.34 | 0.47 |
| 3559.89 | 0.000 | −0.69 | ... | −0.41 | −0.23 | −0.48 | −1.17 | −0.30 | ... |
| 3580.52 | 0.055 | −0.62 | ... | −0.50 | −0.25 | −0.48 | −1.24 | −0.32 | ... |
| 3616.57 | 0.000 | −0.31 | ... | −0.48 | −0.26 | −0.46 | −1.18 | −0.32 | ... |
| 3616.62 | 0.055 | −1.03 | ... | ... | ... | ... | ... | ... | 0.54 |
| 3633.54 | 0.000 | −0.53 | ... | −0.57 | −0.30 | −0.63 | −1.27 | −0.40 | ... |
| 3692.65 | 0.055 | 0.28 | ... | −0.52 | −0.27 | −0.46 | −1.33 | −0.31 | 0.49 |
| 3729.53 | 0.000 | −0.59 | 0.91 | −0.47 | −0.19 | −0.48 | −1.14 | −0.26 | ... |
| 3781.02 | 0.669 | −0.66 | 1.05 | −0.42 | −0.23 | −0.38 | ... | −0.24 | ... |
| 3786.84 | 0.000 | −0.52 | 0.98 | −0.47 | −0.20 | ... | −1.09 | −0.29 | 0.59 |
| 3797.06 | 0.055 | −1.03 | ... | −0.42 | ... | −0.41 | ... | −0.25 | ... |
| 3830.48 | 0.000 | −0.22 | 0.86 | −0.52 | −0.24 | −0.53 | −1.22 | −0.35 | 0.64 |
| 3880.61 | 0.636 | −0.25 | ... | −0.49 | −0.21 | −0.48 | −1.16 | −0.30 | ... |
| 3896.23 | 0.055 | −0.12 | 0.97 | −0.49 | −0.23 | −0.58 | −1.28 | −0.29 | 0.52 |
| 3906.31 | 0.000 | 0.12 | ... | −0.47 | −0.21 | −0.33 | −1.16 | −0.32 | 0.64 |
| 3974.72 | 0.055 | −0.85 | ... | −0.40 | ... | ... | ... | ... | ... |
| 4142.91 | 0.636 | −0.72 | ... | −0.46 | −0.28 | ... | ... | −0.27 | ... |
| Er: mean | ... | ... | 0.96 | −0.48 | −0.25 | −0.47 | −1.22 | −0.30 | 0.57 |
| Er: error | ... | ... | 0.02 | 0.01 | 0.01 | 0.02 | 0.02 | 0.01 | 0.02 |
| Er: σ | ... | ... | 0.06 | 0.04 | 0.04 | 0.08 | 0.07 | 0.04 | 0.07 |
| Er: number of lines | ... | ... | 8 | 21 | 17 | 14 | 15 | 19 | 9 |
| Er: median | ... | ... | 0.98 | −0.48 | −0.24 | −0.48 | −1.22 | −0.30 | 0.59 |
| Eu: mean | ... | ... | 0.52 | −0.95 | −0.67 | −0.86 | −1.63 | −0.72 | −0.07 |
| Eu-Er | ... | ... | −0.44 | −0.47 | −0.42 | −0.40 | −0.41 | −0.42 | −0.64 |
| Eu-Er | solar-*r* | ... | −0.37 | ... | ... | ... | ... | ... | ... |

STR $= -0.6$ and increasing it by a factor of 20, or STR $= -0.6 + 1.3 = +0.7$. Ignoring curve-of-growth saturation effects would imply that log (RW) $= -6.5 + 1.3 = -5.2$ (or EW $\approx$ 30 mÅ near 4500 Å). Such lines actually are slightly saturated, and tests with the solar spectrum suggested log (RW) $\approx -5.35$, or EW $\approx$ 20 mÅ at 4500 Å for STR $= +0.7$. We have drawn dashed horizontal lines to indicate this "strong-line" limit in Figure 7.

This study has reported transition probabilities of Er II lines with wavelengths nearly as long as 20,000 Å (2 μm), but Figure 7 displays only the regime 2900 Å $\leq \lambda \leq$ 6000 Å. This is because all of the Er II lines beyond 6000 Å have STR $< -1.7$, more than 1 dex weaker than our estimated minimum detectability threshold of STR $= -0.6$. In fact, the right panel of this figure shows that very few Er II lines should even be detectable in the solar spectrum longward of 4000 Å. We have drawn vertical lines at 4000 Å in the figure to bring attention to this difficulty. Nearly 75 Gd II lines longward of 4000 Å have STR $\geq -0.6$, while just 6 Er II lines qualify. All strong Er II lines are located in the complex near-UV spectral domain, where line blending from other species might compromise even the most promising Er II transition.

As discussed in Lawler et al. (2007) and earlier papers, the strength factors of Figure 7 provided the first cut in paring the list of 418 Er II lines to a useful set for solar/stellar work. Some 115 lines survived the STR $\geq -0.6$ test. We then followed the procedure of Lawler et al. to identify the final set of potentially useful Er II lines. Using the Delbouille et al. (1973) solar center-of-disk spectrum, the Moore et al. (1966) solar line identifications, the comprehensive Kurucz (1998)[12] atomic and molecular line lists, and the spectrum of the *r*-process-rich metal-poor giant star CS 22892−052 (Sneden et al. 2003), we eliminated all but 57 Er II lines; the rest proved to be too weak and/or too blended (see Lawler et al. 2006 for specific examples of the process). The CS 22892−052 spectrum was especially helpful in this exercise, as the combined effects of its very low metallicity ([Fe/H] $\approx -3.1$) and large neutron-capture *r*-process excess (e.g., [Eu/Fe] $\approx +1.6$) creates very favorable conditions for Er II line detection. If a candidate line is unusable in the CS 22892−052 spectrum, it almost certainly will not be available for a solar analysis.

We then computed preliminary synthetic spectra for the surviving Er II lines. As in Lawler et al. (2006), we assembled atomic and molecular line lists in small (4–6 Å) wavelength regions, beginning with the Kurucz (1998) line database and the Moore et al. (1966) solar identifications. For many neutron-capture ionized species we used *gf*-values from recently published studies: Y: Hannaford et al. (1982); Zr: Malcheva et al. (2006); La: Lawler et al. (2001a); Ce: Palmeri et al. (2000); Nd: Den Hartog et al. (2003); Sm: Lawler et al. (2006); Eu: Lawler et al. (2001b); Gd: Den Hartog et al. (2006); Tb: Lawler et al. (2001c); Dy: Wickliffe et al. (2000); Ho: Lawler et al. (2004); Er: the present paper; Hf: Lawler et al. (2007). We adopted the Holweger & Müller (1974) solar empirical model photosphere, and the CS 22892−052 model interpolated from the Kurucz grid by Sneden et al. (2003). For solar computations we used a standard solar abundance set

[12] Available at http://kurucz.harvard.edu.

(e.g., Grevesse & Sauval 1998; 2002; Lodders 2003), modified to include recent updates for the neutron-capture elements, and for CS 22892−052 we used abundances from Sneden et al. (2003), modified for neutron-capture elements by our previous papers in this series.

Line lists, model atmospheres, and abundance sets were input into the current version of the LTE line analysis code MOOG (Sneden 1973) to generate initial synthetic spectra. Empirical Gaussian broadening functions were applied to smooth the synthetic spectra to match the effects of solar/stellar macroturbulence and spectrograph instrumental profile. Visual inspection of the synthetic/observed spectrum matches were sufficient to reduce the 57 candidate lines to 23 that were suitable for abundance analysis in the Sun and/or CS 22892−052. These transitions were the ones examined in all program stars.

### 3.2. *The Solar Photospheric Erbium Abundance*

We computed multiple synthetic spectra for each Er line region in a more careful manner, trying to account for the details of the solar spectra. As discussed in § 2, Er II lines in the red–IR have detectable hyperfine/isotopic substructure (Fig. 3), but it is negligible for the near-UV lines (e.g., Fig. 2) that we used for solar/stellar abundances. Therefore we treated these lines as single absorbers. The oscillator strengths for atomic lines other than the neutron-capture species referenced in § 3.1 were adjusted to fit the solar spectrum. Abundances of elements C, N, and O were altered to match the strengths of observed CH, CN, NH, and OH lines. Of course many solar absorption features, especially in the near-UV spectral region of greatest interest in this study, remain unidentified. We arbitrarily declared these lines to be Fe I with excitation potentials $\chi = 3.5$ eV and $gf$-values adjusted to fit the solar spectrum. We compared these iterated synthetic spectra to the Delbouille et al. (1973) center-of-disk photospheric spectrum. In any case for which line contamination of identified or unknown origin proved to be a significant part of the overall absorption at the Er II wavelength, the line was discarded for the solar analysis but kept for possible use with the metal-poor giants.

The final solar Er abundance is based on eight Er II lines, whose individual abundances are listed in Table 4, column (4). These lines include the 3896.2 Å feature identified by Moore et al. (1966), but their 3903.3 Å line was not part of our laboratory investigation. In the top panel of Figure 8 we display the solar Er line abundances; no obvious trends with wavelength are apparent. A straight mean abundance is $\log \varepsilon(\mathrm{Er}) = 0.96 \pm 0.02$ ($\sigma = 0.06$).

Abundance uncertainties have been described in earlier papers of this series. Here, we estimate line profile fitting uncertainties to be ±0.02 dex, and uncertainties due to contamination by other species lines are ±0.04 dex. The mean error in log ($gf$) for the eight lines used in the solar analysis (see Table 3) is ±0.02. Adding these uncertainties in quadrature yields an estimated total internal uncertainty per transition of ±0.05 dex, which is close to the observed $\sigma = 0.06$.

Overall scale errors can be due to atomic data uncertainties beyond $gf$ errors and to model atmosphere choices. Recalling that Saha-fraction corrections are negligible for Er II, the main atomic uncertainties would be Boltzmann factors, which vary with the partition functions. Irwin (1981) computed polynomial fits to partition functions that were generated with the atomic energy level data available at that time, and his formulae have been widely used in stellar line analysis programs. We recalculated Er I and Er II partition functions with the most recent experimental energy level data (Martin et al. 1978, 2000), and found that the new values of log ($U$) are up to ∼0.2 dex larger in the temperature domain of interest for this study. We have used the new partition functions from experimental energy levels for all of our abundances. A reanalysis of Er II, which is currently underway (J. F. Wyart et al. 2008, in preparation), indicates that the remaining unobserved low-lying levels of each parity could further increase the partition function by 0.016 dex at 6000 K, but much less at lower temperature. This final theoretical correction to the Er II partition function is not included here because nearly all of the rare-earth partition functions need similar adjustments due to unobserved levels.

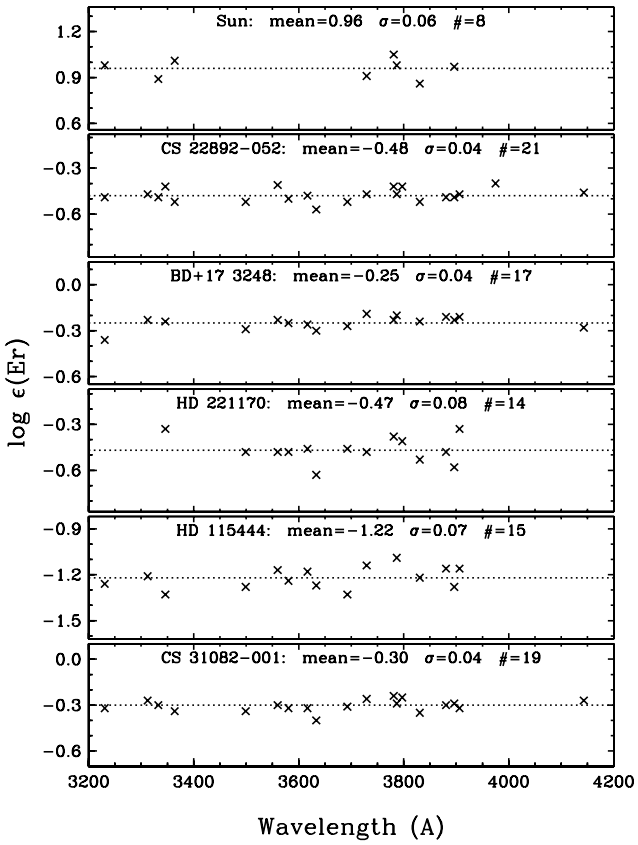


FIG. 8.—Line-by-line Er abundances for the Sun and the $r$-process-rich metal-poor giant stars CS 22892−052, BD +17 3248, HD 221170, HD 115444, and CS 31082−001, plotted as a function of wavelength. For each star, a dotted line is drawn at the mean abundance. As indicated in the figure legend, the three numbers in parentheses beside each star name are the mean abundance, the sample standard deviation $\sigma$, and the number of lines used in the analysis. The small scatter with an increased number of lines in comparison to earlier work (see text) yields improved accuracy and precision of abundance values.

As in Lawler et al. (2007), we repeated some of the abundance computations using the Kurucz (1998) and Grevesse & Sauval (1999) models, finding on average abundance shifts of −0.02 dex compared to those done with the Holweger & Müller (1974) model. Combining line-to-line scatter uncertainties (±0.02 from the standard deviation of the mean, Table 4) with scale uncertainties, we recommend $\log \varepsilon(\mathrm{Er})_{\mathrm{Sun}} = +0.96 \pm 0.03$.

Biémont & Youssef (1984) provided the previous major solar Er investigation. From an equivalent width analysis of seven lines, they derived $\log \varepsilon(\mathrm{Er})_{\mathrm{Sun}} = +0.93 \pm 0.06$, in good agreement with our new value (only the 3781.0 and 3896.2 Å lines are in common between the two studies). Lodders (2003) adopts this abundance in her solar abundance review, and recommends a meteoritic value in even closer agreement with our value: $\log \varepsilon(\mathrm{Er}) = +0.95 \pm 0.03$. This point is considered again in § 4.

In Figure 9 we compare solar system meteoritic abundances with photospheric abundances for the nine rare-earth elements

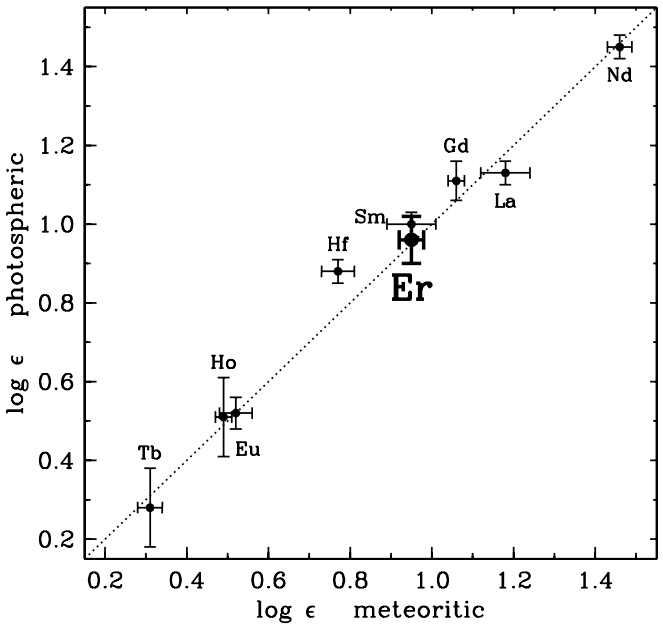


FIG. 9.—Correlation of solar-system meteoritic and photospheric abundances for rare-earth elements studied in this series. The meteoritic abundances and their error estimates are those recommended by Lodders (2003). The sources of the photospheric abundances are La: Lawler et al. (2001a); Nd: Den Hartog et al. (2003); Sm: Lawler et al. (2006); Eu: Lawler et al. (2001b); Gd: Den Hartog et al. (2006); Tb: Lawler et al. (2001c); Ho: Lawler et al. (2004); Er: this study; Hf: Lawler et al. (2007). Error bars adopted for the photospheric abundances are the sample standard deviations reported in those papers, which should be consulted for more detailed assessments. The dotted line indicates equality of the meteoritic and photospheric values. Note that a recently proposed renormalization by Grevesse et al. (2007) would decrease the meteoritic abundances uniformly by 0.03 dex.

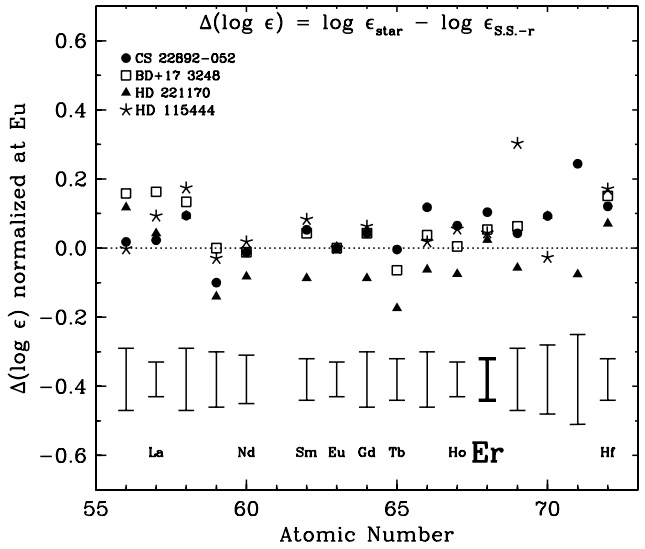


FIG. 10.—Comparison of rare-earth abundances in four *r*-process-rich stars to the solar-system *r*-process-only abundances. The solar-system values are taken from Simmerer et al. (2004). The stars, identified in the figure legend, are those that have been analyzed in this series of papers. For each star, the abundance differences have been normalized such that $\Delta(\log \varepsilon(\mathrm{Eu})) = 0$. The dotted line indicates equality between the stellar and solar-system *r*-only abundances. The error bars are the means of the sigma values of individual stellar abundances. The abundances for the named elements are taken from the present and earlier papers of this series, and other abundances are taken from the original stellar analyses of the stars.

studied in this series of papers. The meteoritic values are adopted from the Lodders (2003) compilation. References to the photospheric values are given in the figure caption. It is clear that the two data sets agree well: a simple mean offset is $+0.01 \pm 0.02$ ($\sigma = 0.05$). These numbers are consistent with error estimates on individual meteoritic and photospheric abundances.

### 3.3. *Erbium Abundances in Five r-Process-rich Low-Metallicity Stars*

We also derived Er abundances in five very metal-poor, *r*-process-rich giant stars: CS 22892−052 ([Fe/H] = −3.1, [Eu/Fe] = +1.5, Sneden et al. 2003); BD +17 3248 ([Fe/H] = −2.1, [Eu/Fe] = +0.9, Cowan et al. 2002); HD 221170 ([Fe/H] = −2.2, [Eu/Fe] = +0.8, Ivans et al. 2006); and HD 115444 ([Fe/H] = −2.9, [Eu/Fe] = +0.8, Westin et al. 2000); CS 31082−001 ([Fe/H] = −2.9, [Eu/Fe] = +1.7, Hill et al. 2002). Many Er II lines that are too blended and/or weak in the solar spectrum could be employed here, and we ended up with 14–21 lines contributing to the mean abundances. We derived Er abundances for the stars in the same manner as was described for the Sun in § 3.2. The abundances from individual lines are listed in Table 4 and displayed in Figure 8. The mean abundances, standard deviations, and number of lines are given at the bottom of Table 4 and Figure 8. The line-to-line scatters are all small, $\sigma = 0.04$–$0.08$. The derived Er abundances show no noticeable dependence on wavelength, log ($gf$), or excitation potential.

## 4. DISCUSSION

The Er results are similar to those found for other RE studies, where the new experimental atomic data have dramatically reduced the scatter in star-to-star elemental abundance comparisons. We show this agreement and these comparisons in Figure 10. In the main portion of the figure we show the differential elemental abundance values for the four stars CS 22892−052, BD +17 3248, HD 221170, and HD 115444. In all cases the stars' elemental abundances have been scaled relative to Eu and the differences are with respect to the predicted solar system *r*-process only value. For all cases we have employed the *r*-process predictions from Simmerer et al. (2004; see also Sneden et al. 2008). (A perfect agreement with the *r*-process only would fall on the dotted horizontal line in Fig. 10.) Previous studies of the RE elements, including that of Nd (Den Hartog et al. 2003), Ho (Lawler et al. 2004), Sm (Lawler et al. 2006), and Gd (Den Hartog et al. 2006) and of the interpeak element Hf (Lawler et al. 2007), have improved the precision of the stellar elemental abundances, as is apparent by the close agreement in the figure. The Er abundances for these four studied stars now are tightly clustered with relatively small error bars indicated in the bottom of the figure (as means of the sigmas for each element in the four stars) and are consistent with the solar system *r*-process only value.

Table 4 includes analyses for two additional stars. While not included in Figure 10 we have also analyzed the Er abundances in CS 31082−001. Previously we had determined the Hf abundance in this star (see Lawler et al. 2007). From 19 Er II lines we derive $\log \varepsilon(\mathrm{Er}) = -0.30 \pm 0.01$ ($\sigma = 0.04$). With our own analysis of Eu II lines (Lawler et al. 2007) we find $\log \varepsilon(\mathrm{Eu}) = -0.72$, and $\log \varepsilon(\mathrm{Eu/Er}) = -0.42$. This value is essentially identical to the Eu/Er ratios found for the four other *r*-process-rich stars. A more complete analysis is underway (I. I. Ivans et al. 2008, in preparation). In contrast to these *r*-process-rich stars we have also measured nine Er II lines in the star CS 29497−030, a star rich in both *r*- and *s*-process material (Ivans et al. 2005). We find $\log \varepsilon(\mathrm{Er}) = +0.57 \pm 0.02$ ($\sigma = 0.07$), or $\log \varepsilon(\mathrm{Eu/Er}) = -0.64$. The 0.2 dex difference in the ratio between this star and the other five stars results from the effects of changing from a pure *r* abundance to a mix of *r*+*s*.

Interestingly, it appears that the average Er abundance for the four *r*-process-rich stars illustrated in Figure 10 lies just slightly above the scaled solar value. This might suggest that Er may be similar to the cases of Gd (Den Hartog et al. 2006) and Hf (Lawler et al. 2007), where the stellar data argue for a somewhat larger *r*-process fraction for the total solar system abundances (see also Sneden et al. 2008). Some of the remaining small systematic uncertainties, for example, the correction of partition functions for unobserved levels, will further enhance the *r*-process abundances.

A few RE elements remain to be improved including Ce (J. E. Lawler et al. 2008, in preparation), but most of these elements have now been well studied. The Er results presented here, along with the other RE studies, have all led to much more precise stellar elemental abundances. These abundances in the metal-poor (*r*-process-rich) halo stars are all consistent with a solar system *r*-process only origin. This study has further strengthened the finding that *r*-process nucleosynthesis in the early Galaxy, which enriched these metal-poor stars, yielded a very similar pattern to the *r*-process, which enriched later stars including the Sun. This in turn provides important constraints on the timescales for such synthesis—that is it suggests rapidly evolving astronomical sites, forming the elements, ejecting them and mixing them into the interstellar medium, all prior to the formation of the halo stars—and points to the (possibly massive) nature of the first stars.

This work has been supported by the National Science Foundations through grants AST 05-06324 to J. E. L. and E. D. H., AST 06-07708 to C. S., and AST 07-07447 to J. J. C.

REFERENCES

Adams, D. L., & Whaling, W. 1981, J. Opt. Soc. Am. A, 71, 1036
Bentzen, S. M., Nielsen, U., & Poulsen, O. 1982, J. Opt. Soc. Am. A, 72, 1210
Biémont, E., & Youssef, N. Y. 1984, A&A, 140, 177
Biémont, E., & Quinet, P. 2003, Phys. Scr., 105, 38
Brault, J. W. 1976, J. Opt. Soc. Am. A, 66, 1081
Burris, D. L., Pilachowski, C. A., Armandroff, T. E., Sneden, C., Cowan, J. J., & Roe, H. 2000, ApJ, 544, 302
Cayrel, R., et al. 2001, Nature, 409, 691
Cowan, J. J., Sneden, C., Truran, J. W., & Burris, D. L. 1996, ApJ, 460, L115
Cowan, J. J., et al. 2002, ApJ, 572, 861
Danzmann, K., & Kock, M. 1982, J. Opt. Soc. Am. A, 72, 1556
Delbouille, L., Roland, G., & Neven, L. 1973, Photometric Atlas of the Solar Spectrum from $\lambda$ 3000 to $\lambda$ 10000 (Liège: Univ. de Liège Inst. d'Ap.)
Den Hartog, E. A., Lawler, J. E., Sneden, C., & Cowan, J. J. 2003, ApJS, 148, 543
———. 2006, ApJS, 167, 292
Edlén, B. 1953, J. Opt. Soc. Am. A, 43, 339
Frebel, A., Christlieb, N., Norris, J. E., Thom, C., Beers, T. C., & Rhee, J. 2007, ApJ, 660, L117
Grevesse, N., & Sauval, A. J. 1998, Space Sci. Rev., 85, 161
———. 1999, A&A, 347, 348
———. 2002, Adv. Space Res., 30, 3
Grevesse, N., Asplund, M., & Sauval, A. J. 2007, Space Sci. Rev., 130, 105
Grigoriev, I. S., & Melikhov, E. Z. 1997, in Handbook of Physical Quantities (Boca Raton: CRC Press), 516
Hannaford, P., Lowe, R. M., Grevesse, N., Biemont, E., & Whaling, W. 1982, ApJ, 261, 736
Hashiguchi, S., & Hasikuni, M. 1985, J. Phys. Soc. Japan, 54, 1290
Hill, V., et al. 2002, A&A, 387, 560
Holweger, H., & Müller, E. A. 1974, Sol. Phys., 39, 19
Irwin, A. W. 1981, ApJS, 45, 621
Ivans, I. I., Simmerer, J., Sneden, C., Lawler, J. E., Cowan, J. J., Gallino, R., & Bisterzo, S. 2006, ApJ, 645, 613
Ivans, I. I., Sneden, C., Gallino, R., Cowan, J. J., & Preston, G. W. 2005, ApJ, 627, L145
Kurucz, R. L. 1998, in IAU Symp. 189, Fundamental Stellar Properties: The Interaction between Observation and Theory, ed. T. R. Bedding, A. J. Booth, & J. Davis (Dordrecht: Kluwer), 217
Lawler, J. E., Bonvallet, G., & Sneden, C. 2001a, ApJ, 556, 452
Lawler, J. E., Den Hartog, E. A., Labby, Z. E., Sneden, C., Cowan, J. J., & Ivans, I. I. 2007, ApJS, 169, 120
Lawler, J. E., Den Hartog, E. A., Sneden, C., & Cowan, J. J. 2006, ApJS, 162, 227
Lawler, J. E., Sneden, C., & Cowan, J. J. 2004, ApJ, 604, 850
Lawler, J. E., Wickliffe, M. E., Den Hartog, E. A., & Sneden, C. 2001b, ApJ, 563, 1075
Lawler, J. E., Wickliffe, M. E., Cowley, C. R., & Sneden, C. 2001c, ApJS, 137, 341
Lodders, K. 2003, ApJ, 591, 1220
Malcheva, G., Blagoev, K., Mayo, R., Ortiz, M., Xu, H. L., Svanberg, S., Quinet, P., & Biémont, E. 2006, MNRAS, 367, 754
Martin, W. C., Sugar, J., & Musgrove, A. 2000, NIST Atomic Spectra Database (http://physics.nist.gov/PhysRefData/ASD/index.html)
Martin, W. C., Zalubas, R., & Hagan, L. 1978, Atomic Energy Levels The Rare Earth Elements, NSRDS NBS 60 (Washington: U.S.G.P.O.), 174
Moore, C. E., Minnaert, M. G. J., & Houtgast, J. 1966, The Solar Spectrum 2934 Å to 8770 Å, NBS Monograph 61 (Washington: U.S.G.P.O.)
Musiol, K., & Labuz, S. 1983, Phys. Scr., 27, 422
Palmeri, P., Quinet, P., Wyart, J.-F., & Biémont, E. 2000, Phys. Scr., 61, 323
Rosman, K. J. R., & Taylor, P. D. P. 1998, J. Pure Appl. Chem., 70, 217
Simmerer, J., Sneden, C., Cowan, J. J., Collier, J., Woolf, V. M., & Lawler, J. E. 2004, ApJ, 617, 1091
Smith, V. V., Cunha, K., & Lambert, D. L. 1995, AJ, 110, 2827
Sneden, C. 1973, ApJ, 184, 839
Sneden, C., Basri, G., Boesgarrd, A. M., Brown, J. A., Carney, B. W., Kraft, R. P., Smith, V., & Suntzeff, N. B. 1995, PASP, 107, 997
Sneden, C., Cowan, J. J., & Gallino, R. 2008, ARA&A, in press
Sneden, C., Cowan, J. J., Ivans, I. I., Fuller, G., Burles, S., Beers, T. C., & Lawler, J. E. 2000, ApJ, 533, L139
Sneden, C., Cowan, J. J., & Lawler, J. E. 2003, Nucl. Phys. A, 718, 29
Sneden, C., McWilliam, A., Preston, G. W., Cowan, J. J., Burris, D. L., & Armosky, B. J. 1996, ApJ, 467, 819
Stockett, M. H., Den Hartog, E. A., & Lawler, J. E. 2007, J. Phys. B, 40, 4529
Westin, J., Sneden, C., Gustafsson, B., & Cowan, J. J. 2000, ApJ, 530, 783
Whaling, W., Carle, M. T., & Pitt, M. L. 1993, J. Quant. Spectrosc. Radiat. Transfer, 50, 7
Wickliffe, M. E., Lawler, J. E., & Nave, G. 2000, J. Quant. Spectrosc. Radiat. Transfer, 66, 363
Woolf, V. M., Tomkin, J., & Lambert, D. L. 1995, ApJ, 453, 660
Xu, H.-L., Jiang, H. M., Liu, Q., Jiang, Z. K., & Svanberg, S. 2004, Chinese Phys. Lett., 21, 1720
Xu, H., Jiang, Z., Zhang, Z., Dai, A., Svanberg, S., Quinet, P., & Biémont, E. 2003, J. Phys. B, 36, 1771

*Note added in proof*.—The solar and stellar abundances in Table 4 of this paper were computed with an assumption of strict LTE with a Planck source function. A non-LTE treatment differentiates between pure absorption and scattering. Such computations have been performed with a modified version of the synthesis code. No difference is found for the warm, metal-rich case of the Sun. The average abundance correction in our cool, very metal-poor giants is $\Delta\log(\varepsilon) = -0.11$ over the wavelength range: 3350 Å $\leq \lambda \leq$ 4200 Å. But this correction would apply almost equally well to other rare-earth ions, leaving the relative abundance ratios largely unaffected. A more complete discussion is left to a future paper.